

ASSESSMENT OF STRESS/VOLUME-CONTROLLED SOIL-WATER RETENTION
PROPERTIES OF UNSATURATED SANDY SOILS

by

HAILU AYALEW

Presented to the Faculty of the Graduate School of
The University of Texas at Arlington in Partial Fulfillment
of the Requirements
for the Degree of

MASTER OF SCIENCE IN CIVIL ENGINEERING

THE UNIVERSITY OF TEXAS AT ARLINGTON

August 2013

Copyright © by Hailu Ayalew

All Rights Reserved

ACKNOWLEDGEMENTS

Foremost, I would like to express my sincere gratitude to Dr. Laureano R. Hoyos, for his excellent guidance, encouragement, support and care in the accomplishment of this work. Dr. Hoyos served as my advisor in my entire stay at the university and has provided me a valuable guidance with my coarse works and my thesis. I would like to express my sincere thanks to Dr. Anand Puppala and Dr. Xinbao Yu for their willingness to serve as my committee members and to provide me their valuable advice and suggestion.

I would like to express my deepest appreciation to my wife Loza, who provided me tremendous support to complete my degree. It wouldn't have happened without her patience, understanding and unlimited support. I would like to express my heartfelt thanks to my two little sons, Yakob and Noah for not giving them a considerable fun time in order to complete my school work.

Furthermore, I would also like to extend my special thanks to all my family and friends for their moral support and cooperation in all stages of my work.

July 17, 2013

ABSTRACT

ASSESSMENT OF STRESS/VOLUME-CONTROLLED SOIL-WATER RETENTION PROPERTIES OF UNSATURATED SANDY SOILS

Hailu Ayalew, M.S.

The University of Texas at Arlington, 2013

Supervising Professor: Laureano R. Hoyos

The main objectives of this work are to determine the effect of net normal stress and volume change on the soil-water retention properties of silty sand and clayey sand soils under stressed/volume-controlled conditions; to model soil-water retention parameters under stress/volume-controlled conditions; and to model the effect of higher net normal stress state on the soil-water retention characteristics of these two test soils based on the experimental test results.

In order to investigate the effect of stress/volume change on the soil-water retention characteristics of these two test soils, two test methods were followed: the stress/volume-controlled soil-water characteristic test (Tempe pressure cell test) and the contact filter paper test. The first method uses the concept of axis translation to measure

and control matric suction (up to max. of 15 bars). Axis translation is a technique of translating the origin of matric suction from atmospheric air pressure and negative pore water pressure to atmospheric pore water pressure and positive air pressure. This technique avoids the problem of cavitation, which makes the water phase discontinuous during matric suction measurement. The device has two main components: a pressure panel, which is used to apply pore-air pressure and measure water volume change; and a pressure cell assembly with loading frame, which is used both to retain the test specimen and to control loading and volume change during test. Normal stress is applied using a pneumatic loading piston to simulate field condition while volume change is measured using a dial gauge attached to the load shaft. The volume of water expelled out of the soil specimen is measured using a graduated volume-measuring burette attached to the main panel of this device.

Due to the limited supply of air pressure in the laboratory (800 kPa), it was not possible to assess the full trend of the soil-water characteristic curves (SWCCs) using the data points obtained from the stress/volume-controlled SWCC cell, except for the silty sand soil. For this reason, the contact filter paper technique was used to obtain additional SWCC points at higher suction values. Finally, the points obtained from both the pressure cell and the contact filter paper tests were combined and the defined trend of the SWCCs was observed for a whole range of suction values.

Results obtained from the laboratory tests indicate that the SWCC of clayey sand soil, with volume change consideration, yields a higher air-entry value and a lower desaturation rate when compared with no volume change assumption in the calculation of

volumetric water contents. In contrast, the effect of volume change on the air-entry value of the silty sand soil and other key water retention properties is almost negligible due to the fact that relatively coarser soils may not undergo as much volume change during increased vertical loading compared to fine-grained soils. The SWCCs of both soils showed a consistent shift to the right with higher net normal stresses, which is indicative of an increase in the air-entry value with increasing net normal stress, in agreement with results recently reported by different researchers for purely sandy or clayey soils.

Finally, it was also observed that the pore-size distribution of a test soil has a marked effect on the nature of the corresponding soil-water characteristic curve. The results obtained from SWCC tests on both soils, for each net normal stresses, were plotted accordingly on the same graph to assess this effect.

TABLE OF CONTENTS

ACKNOWLEDGEMENTS	iii
ABSTRACT	iv
LIST OF ILLUSTRATIONS	ix
LIST OF TABLES	xii

Chapter	Page
1. INTRODUCTION.....	1
1.1 Introduction.....	1
1.2 Thesis Objectives	2
1.3 Thesis Organization	3
2. LITERATURE REVIEW	5
2.1 Fundamentals of Soil-water Characteristic Curve.....	5
2.2 Previous Work on Stress/volume-controlled SWCC Testing.....	9
3. TEST SOILS AND STRESS/VOLUME-CONTROLLED SWCC DEVICE.....	15
3.1 Test Soil Characteristics	15
3.1.1. Grain Size Distribution	16
3.1.2. Atterberg Limits.....	18
3.1.3. Specific Gravity	19
3.1.4. Compaction Curve	19
3.2 Stress/volume-controlled SWCC Device	21
4. SAMPLE PREPARATION AND TEST PROCEDURES	24

4.1 General Procedures.....	24
4.1.1 Test Program.....	24
4.1.2 Sample Preparation for Stress/volume-controlled SWCC Device.....	25
4.1.3 Calibration of Pneumatic Loading Piston.....	28
4.1.4 Saturation of Ceramic Disk.....	29
4.2 Contact Filter Paper Technique.....	33
5. TEST RESULTS AND DISCUSSION.....	39
5.1 Introduction.....	39
5.2 Model Fitting of Experimental SWCC Data.....	41
5.2.1 The Brooks and Corey (1964) Model.....	41
5.2.2 The van Genuchten (1980) Model.....	42
5.2.3 The Fredlund and Xing (1994) Model.....	43
5.3 Stress-controlled SWCC Models for Silty Sand and Clayey Sand Soils.	43
5.4 Effect of Volume Change on SWCCs.....	52
5.5 Effect of Change in Net Normal Stress on SWCCs.....	58
5.6 Effect of Pore-Size Distribution on SWCCs.....	62
5.7 Prediction of Stress/volume-controlled SWCCs for Wider Range of Net Normal Stresses.....	64
6. CONCLUSIONS AND RECOMMENDATIONS.....	72
6.1 Conclusions.....	72
6.2 Recommendations.....	73
REFERENCES.....	75
BIOGRAPHICAL INFORMATION.....	77

LIST OF ILLUSTRATIONS

Figure	Page
2.1 Visualization aids of saturated/unsaturated soil mechanics based on the nature of the fluid phases	6
2.2 Extended Mohr-Coulomb failure envelope for unsaturated soils (Fredlund and Rahardjo, 1993)	9
2.3 Typical soil-water characteristic curve showing approximate locations of residual water content θ_r , saturated water content θ_s , and air-entry pressure ψ_b (Lu and Likos, 2004)	12
2.4 Representative soil-water characteristic curves for sand, silt, and clay (Lu and Likos, 2004).....	14
3.1 Particle-size distribution curve for a) silty sand, and b) clayey sand soils	17
3.2 Results from liquid limit test for clayey sand soil	18
3.3 Standard proctor compaction curve for a) Silty sand Soil, and b) clayey Sand soil	20
3.4 Stress/volume-controlled SWCC device.....	22
3.5 Key components of stress/volume-controlled SWCC device.....	23
4.1 Triaxial compaction frame and typical sample after compaction.....	26
4.2 Silty sand specimen cut to fit into the retaining ring.	27
4.3 Saturation of the specimen, (a) placement of filter paper and porous stone, (b) attaching perforated steel frame and (c) inundating in distilled water	28
4.4 Calibration chart of pneumatic loading piston.....	29
4.5 (a) Assembling of SWCC cell, (a) ceramic disks, and (b) specimen in a retaining ring inside the SWCC cell	30
4.6 Water and volume change measuring systems, (a) water volume tubes, and (b) dial gauge.....	33

4.7 Filter paper test, (a) materials needed, (b) placing FP, (c) taping two specimens together.....	36
4.8 Calibration Suction-Water Content Curves for Wetting of Filter Paper (Lu and Likos, 2004).....	37
5.1 Comparisons of SWCC points obtained using the pressure cell and the filter paper test	40
5.2 SWCCs modeled using the Fredlund and Xing, van Genuchten and Brooks and Corey equations for silty sand soil with a) NVC, and b) VC for $\sigma - u_a = 25$ kPa	45
5.3 SWCCs modeled using the Fredlund and Xing, van Genuchten and Brooks and Corey equations for silty sand soil with a) NVC, and b) VC for $\sigma - u_a = 50$ kPa	46
5.4 SWCCs modeled using the Fredlund and Xing, van Genuchten and Brooks and Corey equations for silty sand soil with a) NVC, and b) VC for $\sigma - u_a = 100$ kPa	47
5.5 SWCCs modeled using the Fredlund and Xing, van Genuchten and Brooks and Corey equations for clayey sand soil with a) NVC, and b) VC for $\sigma - u_a = 25$ kPa	48
5.6 SWCCs modeled using the Fredlund and Xing, van Genuchten and Brooks and Corey equations for clayey sand soil with a) NVC, and b) VC for $\sigma - u_a = 50$ kPa	49
5.7 SWCCs modeled using the Fredlund and Xing, van Genuchten and Brooks and Corey equations for clayey sand soil with a) NVC, and b) VC for $\sigma - u_a = 100$ kPa	50
5.8 SWCCs of silty sand soil fitted using the Fredlund and Xing model with both volume change and no volume change consideration for net normal stress of 25 kPa	54
5.9 SWCCs of silty sand soil fitted using the Fredlund and Xing model with both volume change and no volume change consideration for net normal stress of 50 kPa	54
5.10 SWCCs of silty sand soil fitted using the Fredlund and Xing model with both volume change and no volume change consideration for net normal stress of 100 kPa	55

5.11 SWCCs of clayey sand soil fitted using the Fredlund and Xing model with both volume change and no volume change consideration for net normal stress of 100 kPa	56
5.12 SWCCs of clayey sand soil fitted using the Fredlund and Xing model with both volume change and no volume change consideration for net normal stress of 50 kPa	56
5.13 SWCCs of clayey sand soil fitted using the Fredlund and Xing model with both volume change and no volume change consideration for net normal stress of 100 kPa	57
5.14 Effect of net normal stress on SWCCs of silty sand soil fitted using the Fredlund and Xing model for no volumechange case	59
5.15 Effect of net normal stress on SWCCs of clayey sand soil fitted using the Fredlund and Xing model with a) no volumechange and b) volume change consideration.....	61
5.16 Effect of pore-size distribution on SWCCs of SC and SM soils modeled using the Fredlund and Xing (1994) equation with NVCconsideration for $\sigma - u_a = 25$ kPa	63
5.17 Effect of pore-size distribution on SWCCs of SC and SM soils modeled using the Fredlund and Xing (1994) equation with NVC consideration for $\sigma - u_a = 50$ kPa	63
5.18 Effect of pore-size distribution on SWCCs of SC and SM soils modeled using the Fredlund and Xing (1994) equation with NVC consideration for $\sigma - u_a = 100$ kPa	64
5.19 Variation of Fredlund and Xing model parameters with respect to net normal stress for SM soil with no volume change consideration for (a) a parameter, (b) n parameter, and (c) m parameter	67
5.20 Variation of Fredlund and Xing model parameters with respect to net normal stress for SC soil with no volume change consideration for (a) a parameter, (b) n parameter, and (c) m parameter	68
5.21 Theoretical SWCCs modeled using the Fredlund and Xing (1994) equation for a wider range of net normal stresses with NVC consideration for (a) SM soil, sand (b) SC soil.....	70

LIST OF TABLES

Tables	Page
4.1 Summaries of test soil properties and test programs	25
5.1 Summary of SWCC fitting parameters for silty sand and clayey sand soils under a net normal stress of 50 kPa with no volume change consideration	52
5.2 Summary of SWCC fitting parameters for silty sand and clayey sand soils fitted using three model equations under net normal stress of 25, 50 and 100 kPa	64
5.3 Summary of FX SWCC fitting parameters for silty sand clayey sand soils fitted under a net normal stress of 25, 50 and 100 kPa with no volume change (NVC) consideration used to predict hypothetical SWCCs.....	71

CHAPTER 1

INTRODUCTION

1.1 Introduction

Different scientists have defined soil in different ways. Agronomists define soil as any natural body on earth that is capable of growing plants, whereas geologists define soil in regard to its formation. An engineering definition of soil is "all the fragmented mineral material at or near the surface of the earth, the moon, or other planetary body, plus the air, water, organic matter, and other substances which may be included therein" (Spangler and Handy, 1982, p. 67). Soil is an erratic natural material which is composed of mainly three physical phases: soil solids, water and air voids. Engineering problems in soil are generally linked to the proportion of these compositions, the arrangement of the soil particles, the external influence they are subjected to, and some other related issues. Therefore, properly investigating the amount of water present in the soil at different time and the influence of its variation on a specific soil type is a vital important in understanding the properties of the soil and addressing the possible problem that may result due to the variation of water in that particular soil.

In order to study the behavior of water in soil, the general field of soil mechanics is divided into two subdivisions: saturated soil mechanics and unsaturated soil mechanics. The differentiation between saturated and unsaturated soils lies in their phase relationship and in their behavior under different stress conditions. Saturated soil has two phases and the pore water pressure is positive relative to the pore-air pressure, whereas an

unsaturated soil has more than two phases, and the pore water pressure is negative relative to the pore-air pressure (Fredlund and Rahardjo, 1993).

Unsaturated soils with negative pore water pressure are main concerns of unsaturated soil mechanics. The need for studying unsaturated soil mechanics arises due to the fact that most of the world's populations are settled in arid and semi-arid environment where unsaturated soils are a major concern. Most infrastructures in these regions of the world are built above the ground water table and most environmental concerns start near the ground surface. Therefore, properly assessing the constitutive behavior of unsaturated soils, which comprises shear strength, seepage and volume change parameters, is of vital important to address these major concerns in engineering practice. Shear strength phenomena is expressed in terms of suction-stress relationships; whereas seepage and volume change phenomena are expressed in terms of both the soil-water characteristic curve (SWCC) and the hydraulic conductivity characteristic curve. The soil-water characteristic curve (SWCC) is the main subject of concern for this thesis.

1.2 Thesis Objectives

The main objectives of this work are to determine the effect of net stress and volume change on the soil-water retention properties of silty sand and clayey sand soils under stressed/volume-controlled conditions; to model soil-water retention parameters under stress-controlled conditions; and to model the effect of higher net normal stress states on the soil-water retention characteristics of these two test soils based on the experimental results. Specific tasks were performed to:

1. Identify and characterize two kinds of intermediate soils with distinct and contrasting physical properties.
2. Develop an experimental program for each test soil to assess the effect of net external stress and volume change on the soil-water retention properties of these test soils.
3. Model the soil-water retention parameters under stress/volume-controlled conditions for a wider range of net normal stresses based on the test results obtained from experiment.
4. Finally, make a recommendation based on the test results from both soils on future research works in this particular area of study.

1.3 Thesis Organization

The thesis is organized into six chapters. Chapter 1 is an introduction that has given an overview of the thesis and states the main objectives of this work.

In Chapter 2, fundamental concepts of the soil-water characteristic curve are presented by reviewing previous studies regarding the subject topic.

In Chapter 3, a brief description of the basic properties of the test soils and the test methods used to accomplish this thesis are presented. This chapter also gives an overview of the test devices used to accomplish the experimental program.

In Chapter 4, the steps followed to prepare the test specimens and the procedures of both stress/volume-controlled stress/volume-controlled SWCC cell and Filter Paper test methods are presented. It also includes the experimental variables selected to accomplish the objectives of the tests.

Chapter 5 presents all test results and all data plots fitted using different SWCC model equations. The trends of the theoretical SWCCs for both test soils and for a wider range of net normal stresses are also predicted by projecting the corresponding SWCC model parameters from experimentally obtained values. The effect of volume change and net normal stress increase on the SWCCs of both test soils is also discussed under this chapter.

Finally, Chapter 6 summarizes the main conclusions from this thesis work and provides some recommendations for future studies.

CHAPTER 2

LITERATURE REVIEW

2.1 Fundamentals of Soil-Water Characteristic Curve

In order to study the behavior of water in soil the general field of soil mechanics is divided into two subdivisions: saturated soil mechanics and unsaturated soil mechanics. The differentiation between saturated and unsaturated soils lies in a number of ways. First, they differ in their phase relationship. Saturated soil has two phases: soil solids and water. An unsaturated soil has four phases: the soil solids, air, water, and the air-water interface that can be referred to as the contractile skin (Fredlund and Rahardjo, 1993). In saturated soils all the voids are filled with water, whereas in unsaturated soils most of the voids are filled with air and there are two fluid phases: continuous water and continuous air phases. Portion of the soil closer to the ground water table has a continuous water phase and a discontinuous air phase, whereas the portion of the soil region further from the ground water table has a discontinuous water phase and a continuous air phase. Figure 2.1 below illustrates the nature of the fluid phases in both saturated and unsaturated soils.

They also differ in their concept of pore water pressure in relative to the pore-air pressure. In saturated soils the pore water pressure is positive relative to the pore-air pressure. In an unsaturated soil the pore water pressure is negative relative to the pore-air pressure.

				Ground Surface		u		<i>where: u is pore water pressure</i>
				-	0	+		
SOIL	Unsaturated soils	air phase	Dry soil		→			negative pore-water pressure due to surface tension force between the water and soil particle contact
			Discontinuous water phase	Continuous air phase (Air filling most)				
		contractile water-air phase	Two fluid phases		→			
			Discontinuous water phase	Continuous air phase				
	water phase	Capillary fringe		→		hc zone of capillary rise	negative pore-water pressure due to capillary action	
continuous water phase (Water filling most voids)		Discontinuous air phase						
Saturated soils	water phase	Saturated Soils		→		γ_w 1	Positive pore-water pressure	

Figure 2.1 Visualization aids of saturated/unsaturated soil mechanics based on the nature of the fluid phases

The third phenomena by which Saturated and unsaturated soils differ is the state of stresses variables. Saturated soil has one stress state variable, $\sigma-u_w$. The stress state variable in saturated soil is called effective stress, $\sigma' = \sigma-u_w$.

where:

σ' = effective stress

σ = normal stress, and

u_w = pore water pressure

Unsaturated soil has two independent stress state variable, $\sigma-u_a$ and u_a-u_w .

where:

σ = normal stress

u_a = pore-air pressure

u_w = pore water pressure

The first stress state variable of unsaturated soils $\sigma - u_a$, is called the net normal stress and the second stress state variable, $u_a - u_w$, is called the matric suction.

The shear strength of soils is directly related to the stress states of that soil. The shear strength of saturated soils is calculated by the equation:

$$\tau_f = c' + (\sigma_n - u_w) \tan \phi'$$

where:

τ_f = the shear strength of the soil at failure.

c' = effective cohesion of the soil.

σ_n = normal stress.

u_w = pore water pressure

ϕ' = effective friction angle of the soil.

In the above equation, the term $(\sigma_n - u_w)$ is called effective stress for saturated soil.

The effective stress in saturated soil is dependent only on one stress state variables.

Effective stress in an unsaturated soil depends on more than one stress state variable: $(\sigma - u_a)$, and $(u_a - u_w)$. There are different relationships developed to predict the effective stress

in unsaturated soils. The most common one is the one proposed by Bishop's (1959) equation:

$$\sigma' = (\sigma - u_a) + \chi(u_a - u_w)$$

where:

σ = normal stress

u_a = pore-air pressure

u_w = pore water pressure

$\sigma - u_a$ = net normal stress

$u_a - u_w$ = matric suction

χ is a property related to the degree of saturation of the soil. Its value ranges from 0 to 1.

The shear strength of unsaturated soils is given by the extended Mohr-Coulomb's equation as follow:

$$\tau_{ff} = c' + (\sigma_n - u_a) \tan \phi' + (\sigma_n - u_w) \tan \phi^b$$

where:

τ_{ff} = the shear strength of the soil at failure.

c' = effective cohesion of the soil.

σ_n = normal stress.

u_w = pore water pressure

u_a = pore-air pressure

$\sigma - u_a$ = net normal stress

$u_a - u_w$ = matric suction

ϕ' = effective friction angle of the soil.

ϕ^b is the angle the projection of the failure envelope makes from the matric suction axis in the matric suction- shear strength plane as shown in figure 2.2.

Different researchers have reported that the key constitutive modeling parameters of unsaturated soils, which are the shear strength, the seepage and volume change behaviors are highly affected by the suction inside the soil. Fredlund and Morgenstern (1977) introduced an idea how the behavior of unsaturated soils is affected by soil suction and Fredlund and Rahardjo (1993) introduced a concept how an unsaturated soil is affected by matric suction in terms of stress state variables. They reported that the shear strength of an unsaturated soils increase with increase in soil suction and the coefficient of permeability decreases with increase in soil suction.

In order to quantify the shear strength of unsaturated soils it is critical to have a very reliable method of measuring each stress state variable. Different researchers have developed various methods of measuring matric suction. Soil-water characteristic curve of a soil is conventionally measured by means of tensiometer (Cassel and Klute, 1986 and Stannard, 1992), the Fredlund SWCC device (Bocking and Fredlund, 1980), electrical/thermal conductivity sensors (Phene et al. 1971a, 1971b, Fredlund and Wong, 1989), and the contact filter paper test (Houston et al. 1994) are the most common ones. All the techniques, but the Fredlund SWCC device is applicable both in field and in laboratory. The Tensiometer and electrical/thermal conductivity sensors are used for small range suction values. The Fredlund SWCC device method is used for relatively higher values of suction, up to 1,500 kPa and has higher reputability. The contact filter paper method is used for a wide range of suction value up to the interest of the person conducting the test.

The Fredlund SWCC device method of measuring matric suction uses the concept of axis translation. The term "axis translation" refers to the technique where the origin of reference or axis for the matric suction variable is translated from the condition of atmospheric air pressure and negative water pressure to the condition of atmospheric water pressure and positive air pressure (Lu and Likos, 2004). In this technique, the pore water pressure is maintained to be constant at an atmospheric pressure and the pore-air pressure is continuously increased until the soil is dry under a specified suction value. This avoids the problem of water cavitation, which makes the water phase inside the soil discontinues during matric suction measurement due to the negative water pressure.

Soil-water characteristic curve (SWCC) of soils can be constructed following two processes: the wetting and drying processes. There are three parameters of importance from the SWCCs developed either following the desorption or absorption processes. These parameters are; the saturated water content θ_s , which indicates the point on the SWCC where all the soil pores are filled with water, the air-entry pressure ψ_b , which indicates the suction point on the desorption curve where air first starts to enter the soil, and the residual water content θ_r , which indicates the point of water content where it becomes extremely hard to remove water from the soil (Lu and Likos, 2004). Three of these points and the two processes of constructing the SWCCs of soil are described in fig 2.3 below.

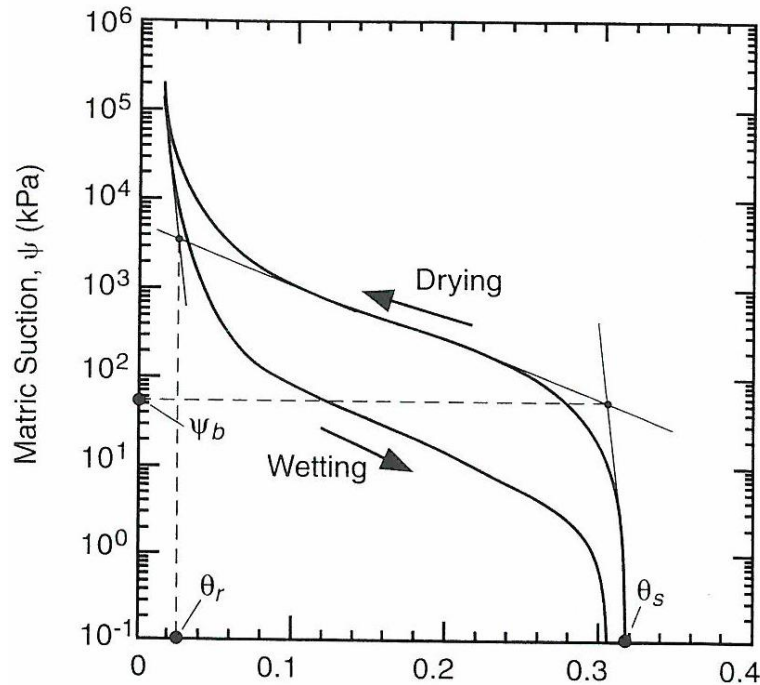


Figure 2.3 Typical soil-water characteristic curve showing approximate locations of residual water content θ_r , saturated water content θ_s , and air-entry pressure ψ_b (Lu and Likos, 2004)

Soil-water characteristic curve (SWCC) is a plot of volumetric water content θ_w and matric suction ($u_a - u_w$), which indicates the configuration of water-filled pores in soil (Lu and Likos, 2004). It is a fundamental constitutive relationship in unsaturated soil mechanics, which describes the relationship between soil suction and soil-water content. It defines the water retention capacity of soils at a particular suction state.

The general behaviors of soil-water characteristic curves are dependent on soil type as shown in fig 2.4 below (Lu and Likos, 2004). Results from this study has shown that soils with larger particles have low specific surface area and have the lowest capacity for water absorption under short range of suction. On the contrary, soils with smaller

particles have higher specific surface area and have the highest water absorption capacity under short range of suction. "Capillarity is the dominant suction mechanism over the majority of the unsaturated water content range, terminating at a relatively low air-entry pressure controlled by the relatively large pore throats formed between and among the soil particles. The overall slope and shape of the capillary regime is controlled primarily by the pore-size distribution of the material."

Soils with a relatively narrow pore-size distribution are marked by relatively flat characteristic curves in the capillary regime because the majority of pores are drained over a relatively narrow range of suction. Soils with a relatively wider pore-size distribution are marked by relatively steeper characteristic curves in the capillary regime because the majority of pores are drained over a relatively wider range of suction. For this reason, the SWCC of clayey soils is characterized with higher air-entry value and shifts to the right compared to the SWCCs of sands and silts which are characterized with lower air-entry value shifting to the left. The behaviors of the SWCCs for sandy, silty and clayey soils are illustrated in the figure below.

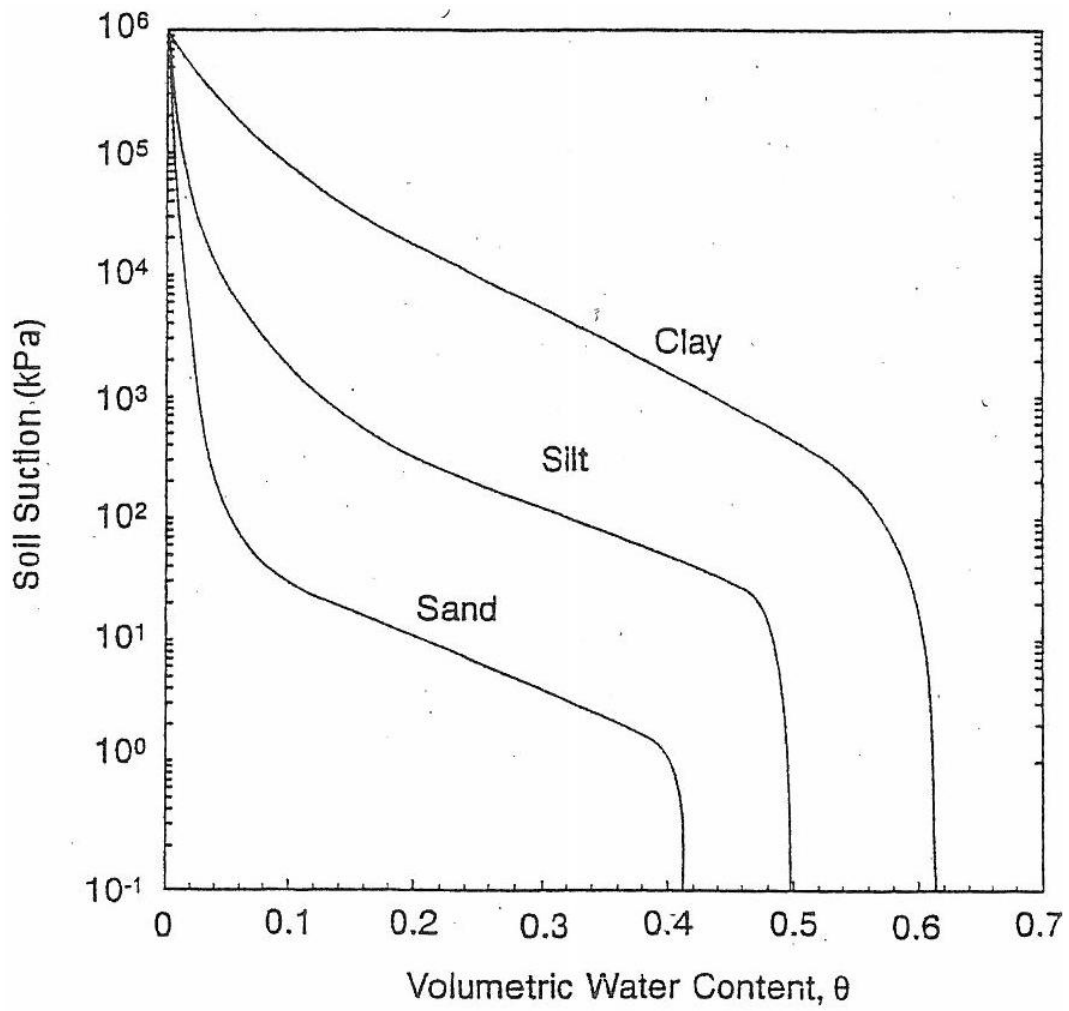


Figure 2.4 Representative soil-water characteristic curves for sand, silt, and clay (Lu and Likos, 2004)

CHAPTER 3

TEST SOILS AND STRESS/VOLUME-CONTROLLED SWCC DEVICE

3.1 Test Soil Characteristics

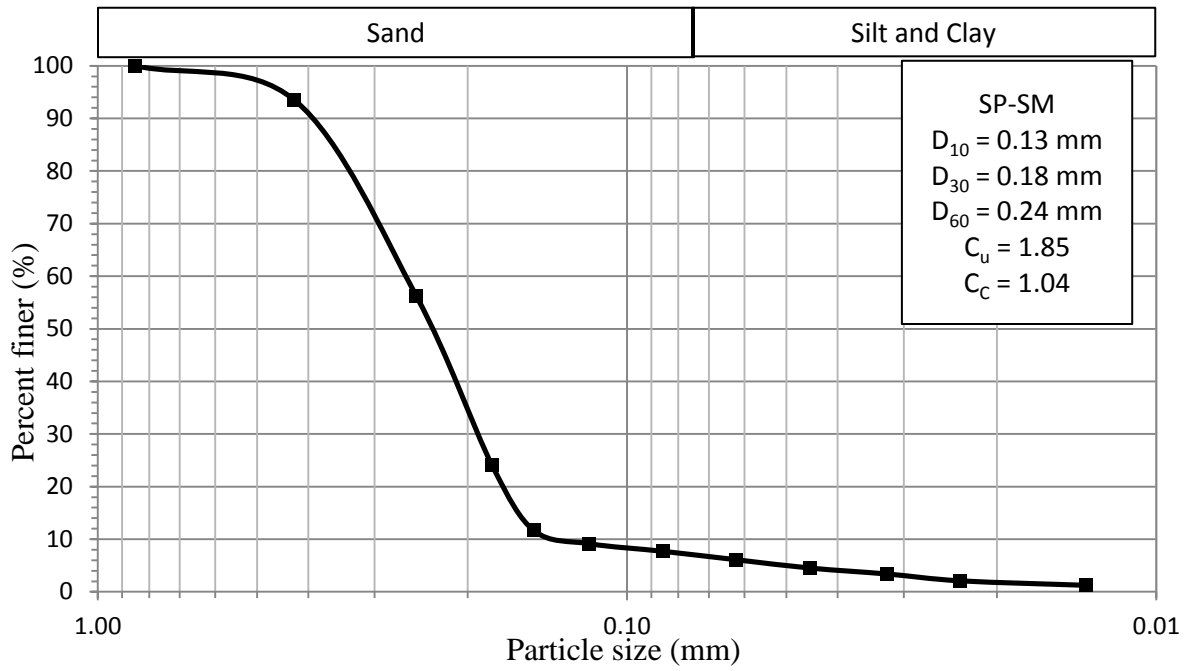
The two types of soils used for this test are silty sand and clayey sand soils. Initially, the test soils were prepared by mixing two different soils together. The silty sand soil is prepared by mixing two separately manufactured silt and sand soils. 60% by weight of the manufactured sand was mixed with 40% by weight of the manufactured silt. After thoroughly mixing the two soils, a gradation test was made for the silt, the sand and the mixture of silt and sand soil. Almost 100% of the sand is retained on sieve No-200 and more than 75% of the silt soil is retained on sieve No-200. Based on the gradation curve, the mixture of the two soils was found to contain 6% by weight of silt and 94% by weight of sand. This indicates that the manufactured silt contains more fine sand in it.

Similarly, the clayey sand soil was prepared by mixing natural clayey sand soil and manufactured sand soil. The manufactured sand soil is the same as the one used for mixing the silty sand soil. After conducting a sieve analysis test for the natural clayey sand soil, it was found that more than 90% of the soil particles are coarser than sieve No-200. The clay soil contains coarse sand and some fine silt in it. The gradation curve for the clayey sand soil shows 8% by weight of clay and 92% by weight of sand. Basic soil classification tests, like sieve analysis test, hydrometer analysis, Atterberg limits, specific

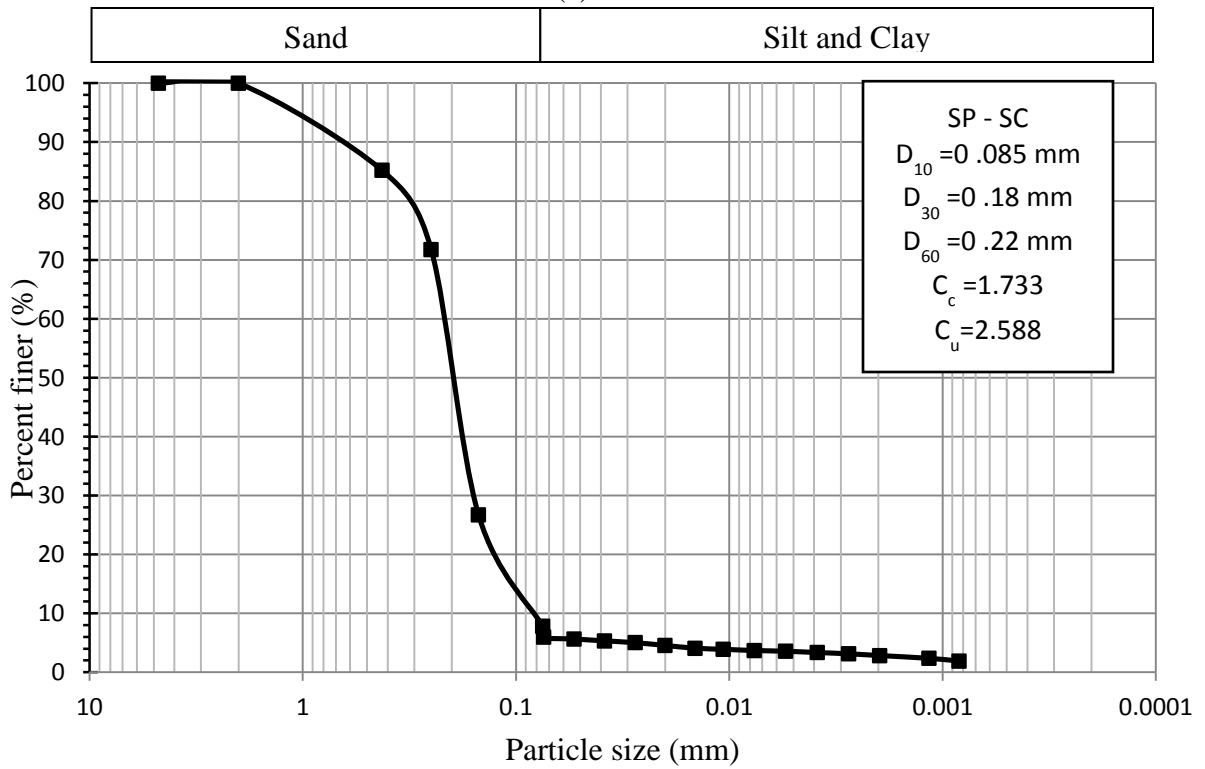
gravity test, and soil compaction tests are performed to characterize the test soils and are presented in the following paragraphs.

3.1.1. Grain Size Distribution

The particle-size distribution test for both test soils was determined by following the procedures set in ASTM D6913 - 04, Standard Test Methods for Particle-Size Distribution (Gradation) of Soils Using Sieve Analysis, and ASTM D6913 for hydrometer test. The sieve analysis test is performed by method B of ASTM D6913 – 04, where a single-set sieving is performed for the soils whose particle-sizes are less than 4.75 μ m. A representative specimen was obtained from the sample, oven dried in an oven capable of maintaining a temperature of $110 \pm 5^{\circ}\text{C}$ for 24 hrs to avoid sample aggregation. The clay soil is then pulverized using a pulverizing machine and oven dried again to remove any moisture gained during the pulverizing operation. The required proportions of soils were mixed and approximately 500gm of mixed sample was taken for the test. Then the soils were sieved using No.4, No.10, No.40, No.60, No.100 and No.200 US standard sieves for 10 minutes. The mass of soil retained in each sieve was then measured. Soil passed through No. 200 sieve during sieving was then used to conduct hydrometer test according to ASTM D6913. Figure 3.1 shows the particle-size distribution curve for both test soils.



(a)



(b)

Figure 3.1 Particle-size distribution curve for a) silty sand, and b) clayey sand soils

3.1.2. Atterberg Limits

Atterberg limits were performed for both test soils following the procedures outlined in ASTM D 4318-10. Method B of this standard on soils passing the 425 μm (No 40) is used. For the silty sand soil, after performing a number of trials, it was not possible to find the water content that closes the gap on the Casagrande cup at 25 blows neither is the soil formed into a thread to perform the plasticity test. With low water content grooving breaks the soil and with higher water content the groove closes way below 25 blows. Cone penetrometer is recommended for this kind of soils to perform the LL. For this reason, it was not possible to perform the PI test using the Casagrande's cup and the soil is reported to be a low PI, non-plastic, poorly graded silty sand soil (SP-SM).

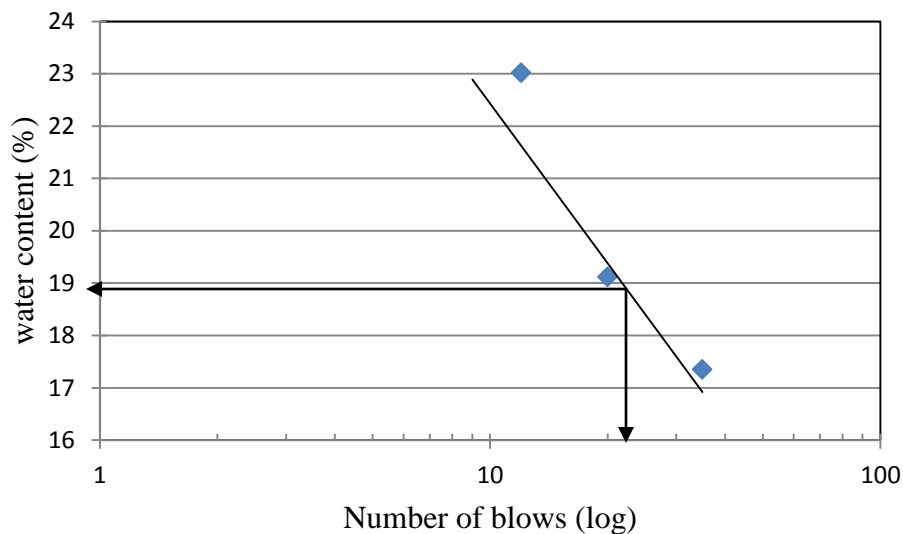


Figure 3.2 Results from liquid limit test for clayey sand soil

As it can be seen from the above plot, the liquid limit of the clayey sand soil is found to be, $LL = 19$. The plastic limit test of this soil was performed following the

procedures set in the same standard as for the silty sand soil above and it was found to be, $PL = 14$. Hence, the plasticity index, PI of the clayey sand soil is equal to:

$$PI = LL - PL = 19 - 14 = 5.$$

Based on the test results, this soil is classified as poorly-graded low PI , non-plastic clayey sand soil ($SP-SC$).

3.1.3. Specific Gravity

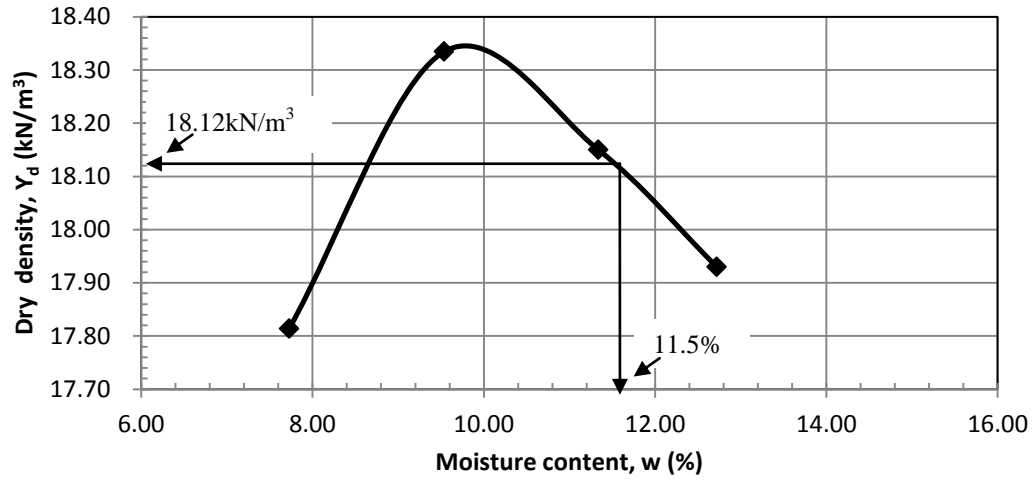
The specific gravity measurements were performed on the fraction of soil passing 4.75-mm (No.4) sieve by the water pycnometer method following the procedures outlined in ASTM D854 -10 standards. Accordingly, the specific gravity values for the two types of soils are: 2.65 for the silty sand soil and 2.69 for the clayey sand soil.

3.1.4. Compaction Curve

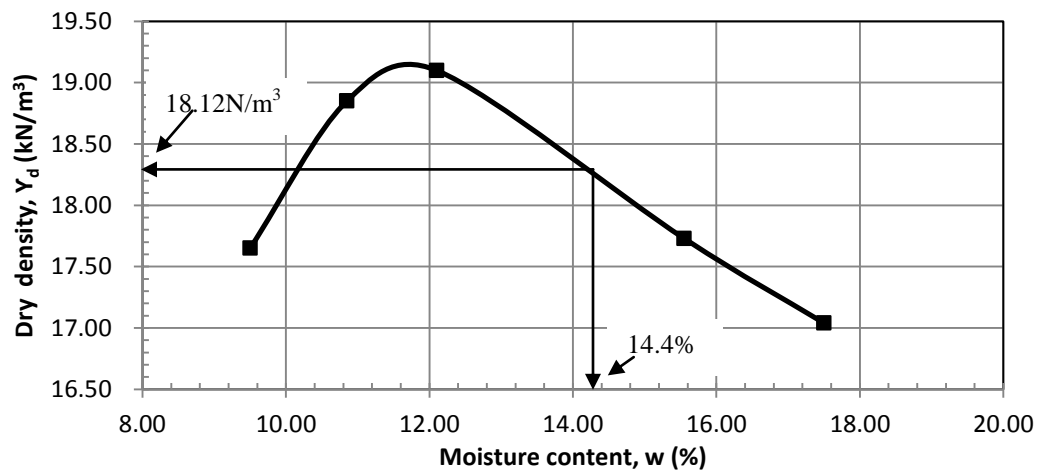
Standard Proctor compaction test was performed according to ASTM D698-12 standard to determine the relationship between moisture content and dry unit weight of the test soils. Based on the test, the optimum moisture content of the silty sand soil is approximately 9.75% with a corresponding dry unit weight of 18.34 kN/m^3 . The moist unit weight of this soil is 20.5 kN/m^3 . The water content at 98.4% of the maximum dry density on the wet side of the compaction curve is used to prepare the test specimen for this soil, which gives a maximum dry unit weight of 18.12 kN/m^3 and moisture content 11.5%, respectively which is presented in figure 3.3(a) below.

Similarly, the optimum moisture content of the clayey sand soil is approximately 11.75% with a corresponding dry unit weight of 19.20 kN/m^3 . The moist unit weight of the soil is 21.5 kN/m^3 . The water content at 95% of the maximum dry density on the wet

side of the compaction curve is used to prepare the test specimen for this soil, which gives a maximum dry unit weight and moisture content of 18.24 kN/m^3 and 14.4% respectively, which is presented in figure 3.3(b) below.



(a)



(b)

Figure 3.3 Standard proctor compaction curve for a) Silty sand Soil, and b)

clayey Sand soil

3.2 Stress/volume-controlled SWCC Device

The SWCC device utilized in the present work is an unsaturated soil testing device which enables to assess the relation between matric suction and water content of the soil while applying one dimensional vertical load (Fredlund 2006). The device is capable of applying matric suction up to a maximum of 1,500 kPa (15 bars) and uses axis translation technique to measure the matric suction of the soil specimen. It has two main components, a pressure panel and a pressure cell assembly with a pneumatic loading frame mounted on it. The pressure panel is used to apply the pore-air pressure while the pressure cell is used to retain the test specimen during the test and control both the vertical load and the volume change experienced by the soil. The loading frame enables to apply a controlled vertical load to simulate the field stress condition of soils. In this particular work, a constant net vertical stress was applied and the corresponding axial deformation was recorded using a dial gauge to predict the effect of vertical stress and volume change on the soil-water retention characteristics of two different test soils. The SWCC test was performed following the drying process of both soils. The complete Fredlund SWCC device is shown below.

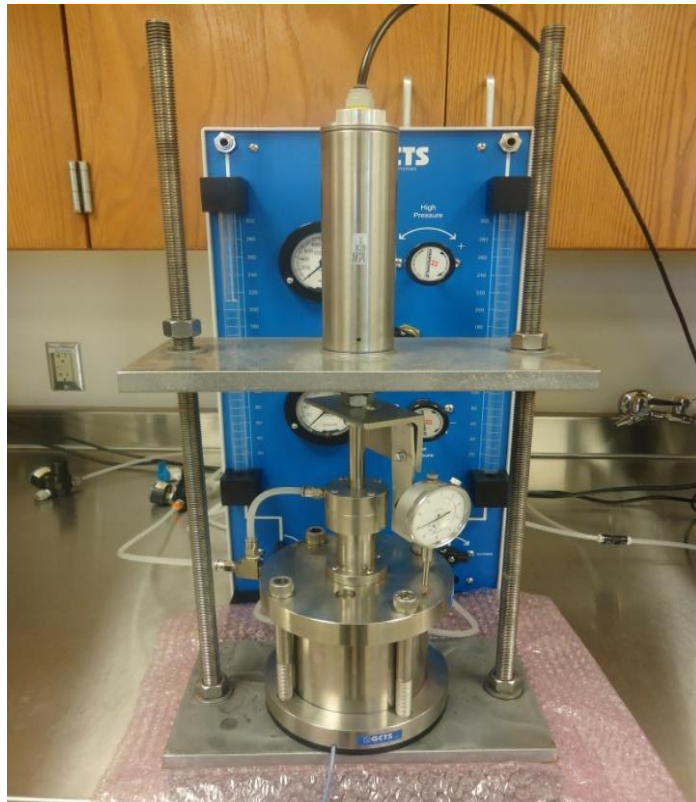


Figure 3.4 Stress/volume-controlled SWCC device

The custom-made stainless steel loading frame and the specimen retaining ring inside the stress/volume-controlled SWCC cell were both manufactured in the UTA's machine shop. The loading frame is used to accommodate the stress/volume-controlled SWCC cell inside the frame and for application of the vertical load through the pneumatic loading piston. The retaining ring was modified to have three legs with a size of 62 mm inside diameter and 23 mm height. The three legs on the retaining ring at its bottom end tightly conform to the inner rigid wall to avoid the chance of eccentricity loading during the test.

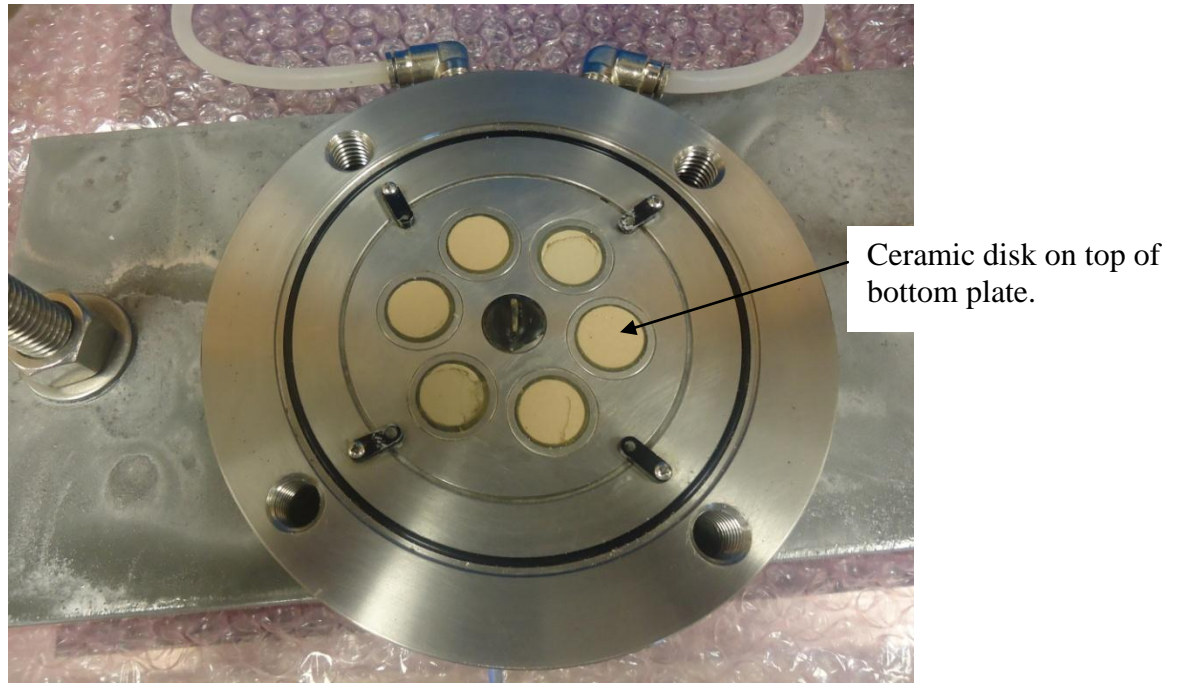


Figure 3.5 Key components of stress/volume-controlled SWCC device

CHAPTER 4

SAMPLE PREPARATION AND TEST PROCEDURES

4.1 General Procedures

4.1.1 Test Program

The purpose of this study is to investigate the soil-water retention characteristics of unsaturated silty sand and clayey sand soils under stress/volume-controlled conditions. The SWCC test was performed following the drying process for both soils (this study doesn't include the suction measurement following the wetting process). The vertical deformation was recorded using a dial gauge which is attached to the loading piston to see the effect of volume change on the SWCC. To identify the influence of net stress state, four different net normal stresses ($\sigma - u_a$) of 0, 25, 50 and 100 kPa were considered. All the samples were prepared with moisture content on the wet side of the compaction curve. Summaries of the test programs and the soil properties used to run the tests are presented in table 4.1.

Table 4.1 Summaries of test soil properties and test programs

Soil properties/test program	Silty sand (SM)	Clayey sand (SC)
γ_d (kN/m ³)	18.34	19.2
w _{opt} (%)	9.75	11.75
γ_m (kN/m ³)	20.5	21.5
Moisture used to prepare specimen (%)	11.5	14.4
Corresponding dry unit weight (kN/m ³)	18.12	18.24
Specific gravity, G _s	2.65	2.69
LL	-	19
PL	-	14
PI	-	5
USCS soil classification	SP-SM	SP-SC
Net normal stress (kN/m ²)	25	25
	50	50
	100	100
Number of test	3	3

4.1.2 Sample Preparation for Stress/volume-controlled SWCC Device

The test specimens for both types of soils were prepared following the same procedures. First, the soil was air-dried for several days, pulverized and passed through US # 10 sieves to avoid the effect of largest particles on the air-entry value of the test specimens. The air-dried soil is then mixed with the desired amount of distilled water to achieve the preferred moisture content and dry density obtained from the compaction curve. After the mixing process is completed, the soil is kept in a humidity controlled room in a plastic bag for at least 48 hours to allow uniform moisture distribution.

All samples for the testing program were statically compacted to 72 mm in diameter and 140 mm in height using a conventional triaxial loading frame (figure 4.1). The samples were prepared in a single layer in a constant volume mould to achieve the

required initial condition of water content and dry density. A compaction displacement rate of 125mm/min was adopted in order to minimize the potential for fabric variations throughout the sample (Venkatarama, 1993).

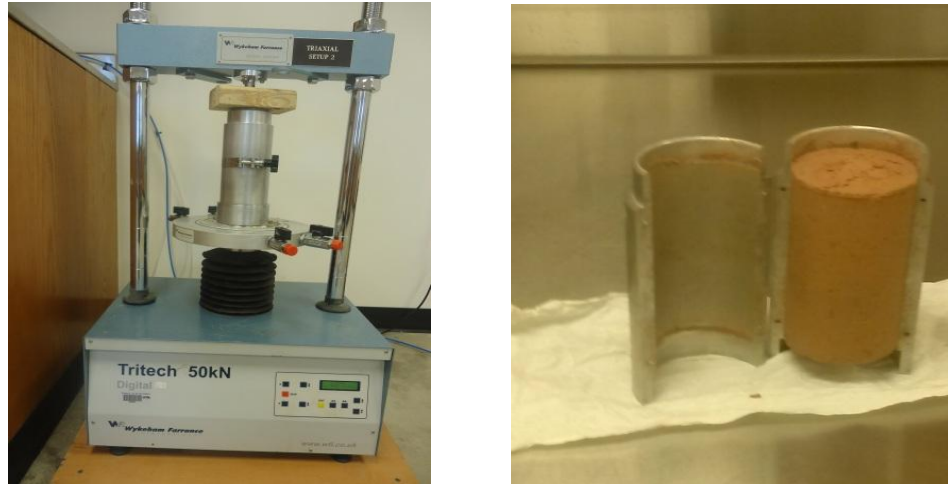


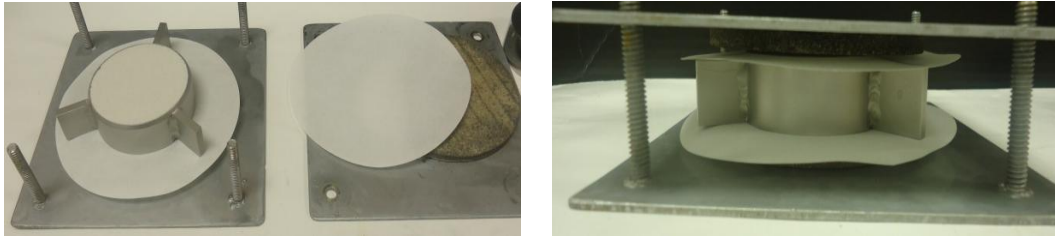
Figure 4.1 Triaxial compaction frame and typical sample after compaction

A specimen of 62 mm in diameter and 23 mm in height was cut from the compacted sample to accommodate into the retaining ring (figure 4.2). Special care should be given during removing of the sample off the compaction mould and during cutting the specimen to accommodate it into the retaining ring not to disturb the initial conditions of the compacted soil.



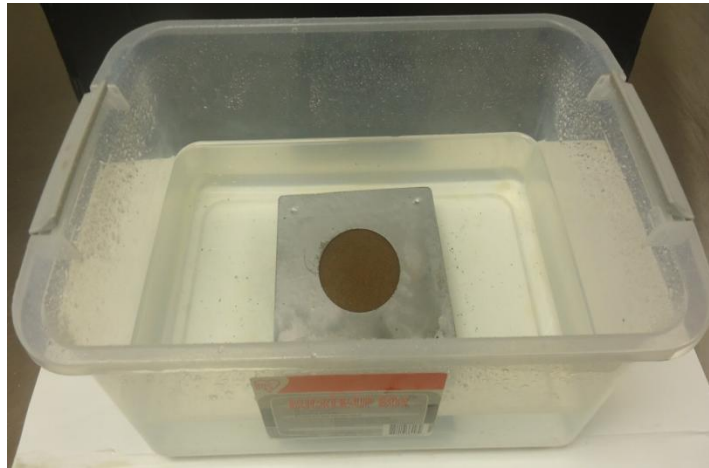
Figure 4.2 Silty sand specimen cut to fit into the retaining ring

The specimen prepared in the retaining ring was then fully immersed in a custom-made saturation chamber filled with distilled water for saturation. Before the start of the saturation process, one filter paper and one porous stone were placed at both ends of the specimen (figure 4.3, a). The porous stones were fixed to the sample with two perforated plates in order to allow drainage at top and bottom and attached by four screws to prevent any volume change (figure 4.3, b) during the saturation process. The specimen is then left submerged in distilled water for three days to allow full saturation (figure 4.3, c).



(a)

(b)



(c)

Figure 4.3 Saturation of the specimen, (a) placement of filter paper and porous stone, (b) attaching perforated steel frame and (c) inundating the specimen in distilled water

4.1.3 Calibration of Pneumatic Loading Piston

Before the start of the test the pneumatic loading piston is calibrated using a load cell (LM 317) supplied by OMEGA. During calibration process, the load cell was attached at the bottom plate of the loading frame and the piston was mounted at the top of the load cell. The top of the piston was connected with the main air supply system of the building through a pressure regulator. Successive increment of air pressure was supplied

using the pressure regulator to the piston and the applied load on the load cell was measured for each increment. Finally, the input pressure (kPa) was plotted against the output load (N) to complete the calibration of the piston which is presented in Figure 4.4 below.

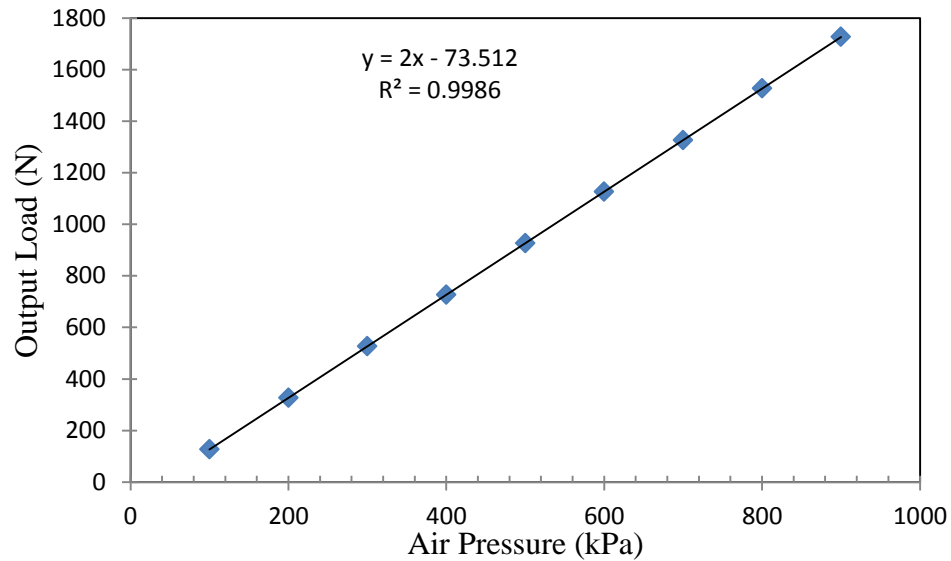


Figure 4.4 Calibration chart of pneumatic loading piston

4.1.4 Saturation of the Ceramic Disk

During the specimen preparation, the ceramic disks (15 bars) in the stress/volume-controlled SWCC cell were saturated before the start of any test and in-between tests in order to wet the ceramic disk and remove any accrued air inside the pores of the ceramic disks. Deaired water is poured on the top of the ceramic disks attached to the bottom plate and the rigid wall is covered with the top plate using screws. Then, an air pressure of 200 kPa was applied to the system and left for 24 hours in order to remove any air bubbles inside the voids of the ceramic disks. During the air pressure application, the connection to the water volume tube at the bottom plate was kept open to allow full

drainage. After saturation is completed, all the water is removed out of the stress/volume-controlled SWCC cell and the ceramic disks are dried.

Once the saturation of the ceramic disks was completed, the saturated specimen with the retaining ring was removed from the water. Any excess water was drained and wiped out from the retaining ring and the specimen with the retaining ring was weighed. Then, the specimen with the retaining ring was placed on top of the ceramic disk which was attached to the bottom plate of the cell. A loading cap was placed on the top of the specimen to apply vertical load from the loading piston. Both the specimen with the retaining ring and the loading plate on the top of the specimen were centered properly to avoid eccentric loading. Then, the top plate was attached with screws to make the cell air tight and the load shaft of the piston with the attached dial gauge was brought into position to apply vertical load (Figure 4.5). Before the test, any possible air leakage of the system was examined thoroughly.



(a)



(b)

Figure 4.5 Assembling of SWCC cell, (a) ceramic disks, and (b) specimen in a retaining ring inside the SWCC cell

After securing the top plate to the bottom plate, the pressure sources were connected to the pressure panel and/or to the respective suction and load applying plastic tubes keeping the pressure valves closed. Then, the right water volume measuring tube was filled with de-aired water until the right tube was full and some volume of water was seen on the left tube. The entire system flushed with de-aired water to remove any air bubbles trapped at the base of the stress/volume-controlled SWCC cell. Only one water volume tube was monitored for water level change and the other one was kept closed during testing except to flush the system. The desired net normal stress (for example 50 kPa) was then applied to the specimen through the piston and left for consolidation until there was no volume change in the specimen. After consolidation was done, the initial air pressure (example $u_a - u_w = 25$ kPa) was applied to the cell and outflow readings were recorded in the water volume tube until no outflow was observed, which indicates that the specimen is in equilibrium with the applied pressure.

However, once the air pressure was applied, the normal stress was also increased to obtain the desired net normal stress. For example, if the desired net normal stress is 50 kPa and the applied air pressure is 50 kPa, than to maintain a constant net normal stress, the total normal stress is increased to 100 kPa. Once equilibrium was established, a higher pressure was applied and outflow readings were monitored. This method only allowed obtaining the SWCC for suctions below 450 kPa because of the limited air pressure supply (800 kPa) in UTA Civil Engineering Laboratory building. As a result,

filter paper technique was used to complete the SWCC curve for the clayey sand specimens.

The change in water content of the sample at each stage of pressure application was calculated by measuring the water volume that passes through the ceramic disk. The water volume tubes were calibrated in order to obtain a linear relationship between each graduation on the volume measuring tube and the corresponding volume of water in millimeters. Accordingly, the water volume change tubes represented a linear measurement in millimeters and a correlation factor is obtained. The change in height of the graduated cylinder was multiplied by this calibration constant to calculate the amount of water expelled during each suction increment. After long testing periods, a diffused air accumulates underneath the ceramics and introduces an error in either the pore water pressure measurements in constant water content tests or in the pore water volume change in drained tests. So, to minimize this error, the system was flushed frequently, at least twice every day.



(a)

(b)

Figure 4.6 Water and volume change measuring systems, (a) water volume tubes, and (b) dial gauge

4.2 Contact Filter Paper Technique

Because of the limited supply of air pressure (800 kPa) in UTA civil engineering laboratory it was not possible to run the SWCC test using the stress/volume-controlled SWCC cell for suction values more than 450 kPa and the whole trend of the SWCC could not be assessed with these suction values for the clayey sand soil. As a result, filter paper technique was used to complete the SWCC curve for the clayey sand specimens. Matric suction was measured by filter paper technique (FP) following the procedures set in

ASTM D5298 - 10, Standard Test Method for Measurement of Soil Potential (Suction) Using Filter Paper.

This procedure for measuring matric suction requires placing three intact oven dried filter papers that has been dried in oven for at least 16hrs; in this case Whatman No.42 filter paper, in-between two soil specimens. The two outer filter papers are used to prevent the internal filter paper from soil contamination and they are not used to measure matric suction, but the internal one is. The two outer filter papers should be slightly larger in size than the internal filter paper to give the middle filter paper full protection.

First, the sandwiched filter papers were placed in intimate contact with the soil specimens. Then, the two pieces of soil specimen were taped using an electrical tape and put in an insulated jar. The jar is sealed properly and taped using the same electric tape used to tape the soil specimens to prevent moisture exchange between the outside and inside of the jar. Then, the sealed jar was placed in an insulated room with a temperature variation of $20 \pm 3^{\circ}\text{C}$ and left there for seven days for suction equilibration.

At the end of the seventh day, the glass jar was removed from the temperature controlled room and the middle filter paper was taken from the jar using a pair of tweezers and placed in a metal container whose cold tare mass has already been determined before. This entire process must be completed in 3 to 5 s. The key to successful measurements of filter paper water content is to minimize water loss during transfer of filter paper from the specimen container and during mass determination prior to oven drying. Observations have been made of 5% or more mass loss due to evaporation during a 5 to 10 s exposure of the filter paper to a room with relative

humidity, Rh , of 30 to 50% (ASTM D5298-10). After transferring the filter paper into the container, the container was immediately closed and the mass of the wet filter paper and the container was determined.

With the lid of the metal container half opened, the container with the filter paper was placed in oven at $110 \pm 5^\circ$ for at least 10 hrs. Before taking the containers from the oven, the lids were closed and the container was left inside the oven for 5 minutes for equilibrium. Then, the container was taken out from the oven, left on an aluminum block for about 20 seconds to cool the container, and the reading of hot container and dry filter paper was taken. The dry filter paper was discarded out and the weight of the dry container was recorded too. The samples were air-dried for a couple of hours until the next desirable water content state was reached and the process was repeated several times until an air dried condition is attained. The filter papers were handled using a pair of tweezers at all stages of the filter paper test in order to avoid contamination and moisture exchange during the handling process.



(a)



(b)



(c)

Figure 4.7 Filter paper test, (a) materials needed, (b) placing FP, (c) taping two specimens together

The moisture content of the filter paper was determined from the water content of the filter paper and the mass of the dry filter paper as:

$$w = \frac{M_w}{W} * 100\%$$

$$M_w = M_{CP} - M_{HP} + M_H - M_C$$

$$M_{FP} = M_{HP} - M_H$$

where:

w = moisture content of filter paper

M_w = mass of water in the filter paper

M_{FP} = mass of dry filter paper

M_{HP} = mass of dry filter paper + hot container

M_{CP} = mass of wet filter paper + cold container

M_C = mass of cold container

M_H = mass of hot container

The matric suction was determined from appropriate calibration curve. Several relationships between the filter paper water content and suction have been developed by different researchers. In the present work, the calibration curve for Whatman N. 42 recommended by ASTM D5298 -10 was used. This calibration curve is presented as follows.

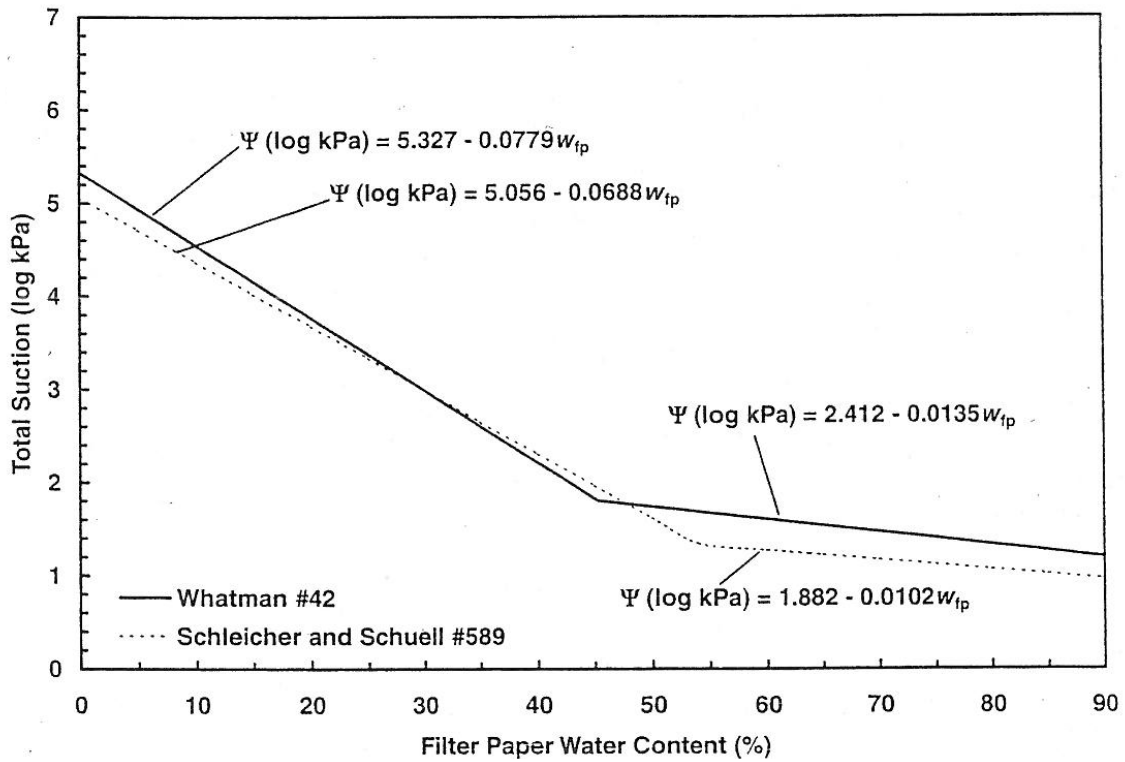


Figure 4.8 Calibration suction-water content curves for wetting of filter Paper (Lu and Likos, 2004)

From the calibration curve above, the following equations were used to determine the matric suction at the corresponding water content:

$$\log (\psi) = 5.327 - 0.0779 w, w < 45.3\%$$

$$\log (\psi) = 2.412 - 0.0135 w, w \geq 45.3\%$$

where,

ψ = matric suction (kPa)

w = filter paper water content (%)

After calculating the moisture content and the corresponding matric suction using the filter paper test, the points were combined with the data points obtained from stress/volume-controlled SWCC device and plotted on the same graph. A divergence between the points obtained from the stress/volume-controlled SWCC cell and the filter paper has been observed, especially at the moisture content where the test specimens are transferred from the stress/volume-controlled SWCC cell to the filter paper method. However, this divergence was reduced at lower moisture content and higher matric suction values. Since filter paper test is very sensitive and requires high laboratory protocol in ensuring an intact contact between the filter paper and the soil specimens, and in avoiding of moisture disruption while handling the filter paper, a slight mistake results in a greater error on the points obtained using this test method. Due to this reason, it has less reputability and its application is limited in soil engineering works. The writer recommends further research to see the difference in the trends of SWCC obtained separately from stress/volume-controlled SWCC cell and filter paper method for the same test soils under similar conditions.

CHAPTER 5

TEST RESULTS AND DISCUSSION

5.1 Introduction

The soil-water characteristic curve is a fundamental constitutive relationship in unsaturated soil mechanics which describes the relationship between soil suction and soil water content. It defines the water retention capacity of soils at a particular suction state. The soil-water characteristic curve (SWCC) of the two test soils for this thesis was determined for different net normal stresses on a specimen prepared on the wet side of the compaction curve in the laboratory using modified stress/volume-controlled SWCC cell. For the silty sand soil, since the soil has relatively coarser particles with low specific area compared to the clayey sand soil, the water inside the soil could be able to drain under a short range of suction, usually under a suction value of less than 1000 kPa. For this reason, the source of air pressure in the Civil Engineering Laboratory was sufficient to obtain enough points to see the full trend of the SWCCs of silty sand soil for all the selected range of net normal stresses.

However, for the clayey sand soil, since its finer clay particle have given it relatively larger surface area compared to the silty sand soil, it has higher water retention capacity and is not possible to drain all its water under short range of suction values. For this reason, it was not possible to finish the SWCC test with the stress/volume-controlled

SWCC cell and it necessitated to run filter paper test to assess the whole tend of the SWCCs.

Two types of tests were performed for the clayey sand soil, the stress/volume-controlled SWCC test and the filter paper test. The test points obtained from both test methods were combined to draw the SWCCs, but some divergence has been observed between the points obtained from both test methods, especially at the transition point as it is seen in fig 5.1 below. Fitting the points obtained from both test methods may create some error in the air-entry value and the residual water content of the soil under test. However this divergence was reduced at higher suction and lower water content values.

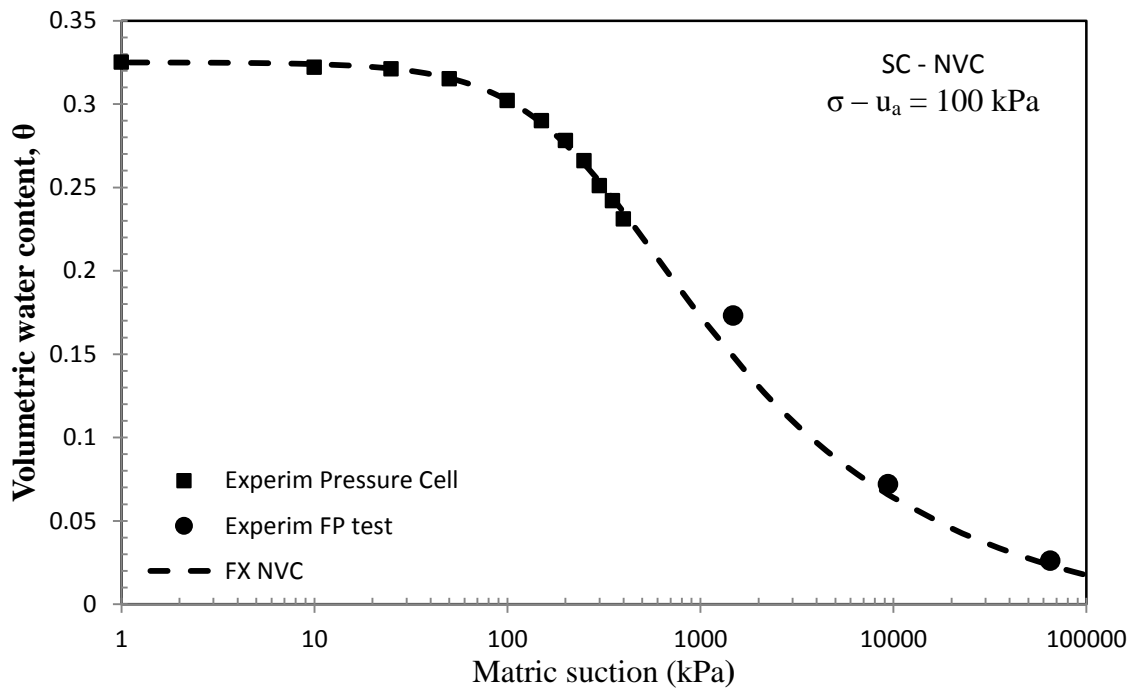


Figure 5.1 Comparison of SWCC points obtained using the pressure cell and the filter paper test methods modeled using the Fredlund and Xing equation for SC soil with no

volume change consideration

The full plots of the SWCCs for both test soils and the models used to fit the experimental data are presented in the following paragraphs.

5.2 Model Fitting of Experimental SWCC Data

Different researchers have provided different types of mathematical equations to best fit the experimental data obtained from direct measurement of the soil-water characteristic curve data. In this work, three of the most frequently used modeling equations in geotechnical field, namely the Brooks and Corey (1964), the van Genuchten (1980), and the Fredlund and Xing (1994) models were used to best fit the experimental data. Each of the equations and model parameters used are described below followed by the plots fitting the experimental data from the test results.

3.1.1 The Brooks and Corey (1964) Model

Based on the Brooks and Corey (1964) model, the volumetric water content of the soil is given by:

$$\theta = \begin{cases} \theta_s & \psi < \psi_b \\ \theta_r + (\theta_s - \theta_r) \left(\frac{\psi_b}{\psi} \right)^\lambda & \psi \geq \psi_b \end{cases}$$

where:

θ = volumetric water content at a given suction value

θ_s = saturated volumetric water content of the soil

θ_r = residual volumetric water content of the soil

ψ_b = the air-entry value of the soil, kPa

ψ = the matric suction of the soil at a given water content, kPa

λ = the pore-size distribution index

5.2.1 The van Genuchten (1980) Model

The van Genuchten model equation is given by:

$$S_e = \left[\frac{1}{1 + (\alpha\psi)^n} \right]^m, \quad \text{and } S_e = \frac{\theta - \theta_r}{\theta_s - \theta_r}$$

where:

θ = volumetric water content at a given suction value

θ_s = saturated volumetric water content of the soil

θ_r = residual volumetric water content of the soil

ψ = the matric suction of the soil at a given water content, kPa

S_e = degree of saturation under fully saturated condition

a , n and m are fitting parameters related to air-entry condition, pore-size distribution, and overall symmetry of the curve, respectively. For simplicity, van Genuchten's m parameter is related to the n parameter by: $m = 1 - 1/n$.

In the above equation if ψ is expressed in units of kPa, the a parameter is expressed in units of kPa^{-1} and replaced by α (Lu and Likos, 2004).

From the above equation, the volumetric water content at any given suction value is calculated as $\theta = S_e (\theta - \theta_r) + \theta_r$.

5.2.2 The Fredlund and Xing (1994) Model

Based on the Fredlund and Xing model the volumetric water content θ is given by:

$$\theta = C(\psi)\theta_s \left[\frac{1}{\ln[e + (\psi/a)^n]} \right]^m$$

where:

θ = volumetric water content at a given suction value

θ_s = saturated volumetric water content of the soil

ψ = the matric suction of the soil at a given water content, kPa

e = the base of the natural logarithmic constant = 2.71828

\ln = the natural logarithm of a number

a , n and m are fitting parameters related to air-entry condition, pore-size distribution, and overall symmetry of the curve, respectively.

$C(\psi)$ = is a correction factor that forces the model through a prescribed suction value of 106 kPa at zero water content and is given by:

$$C(\psi) = \left[1 - \frac{\ln(1 + \psi/\psi_r)}{\ln(1 + 10^6/\psi_r)} \right]$$

ψ_r = the residual matric suction of the soil, kPa

5.3 Stress-controlled SWCC Models for Silty Sand and Clayey Sand Soils

Experimental points obtained from both the stress/volume-controlled SWCC device and the contact filter paper were combined together to plot the SWCCs of the test soils.

Graphical plots of the SWCCs for both test soils fitted using each of the three modeling equations are illustrated in figures 5.2 through 5.7 below.

The following notation with there corresponding terminologies were used throughout the thesis as a short hand form to represent words or phrases in the graphs.

VC – volume change

NVC –no volume change

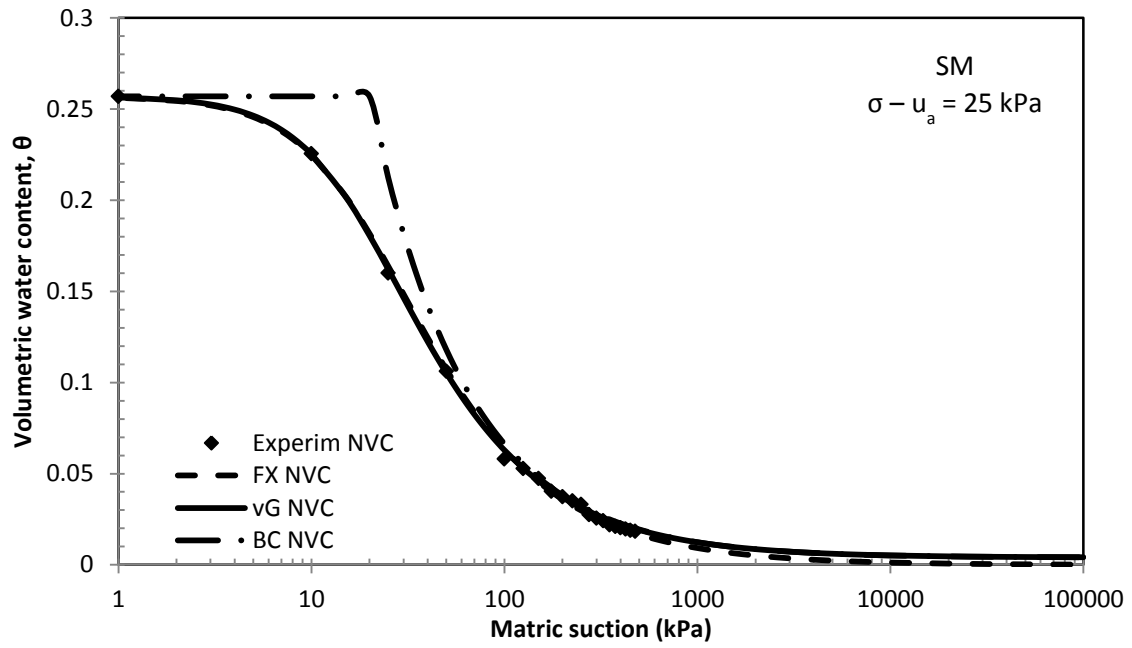
FX – Fredlund and Xing model

vG – van Genuchten model

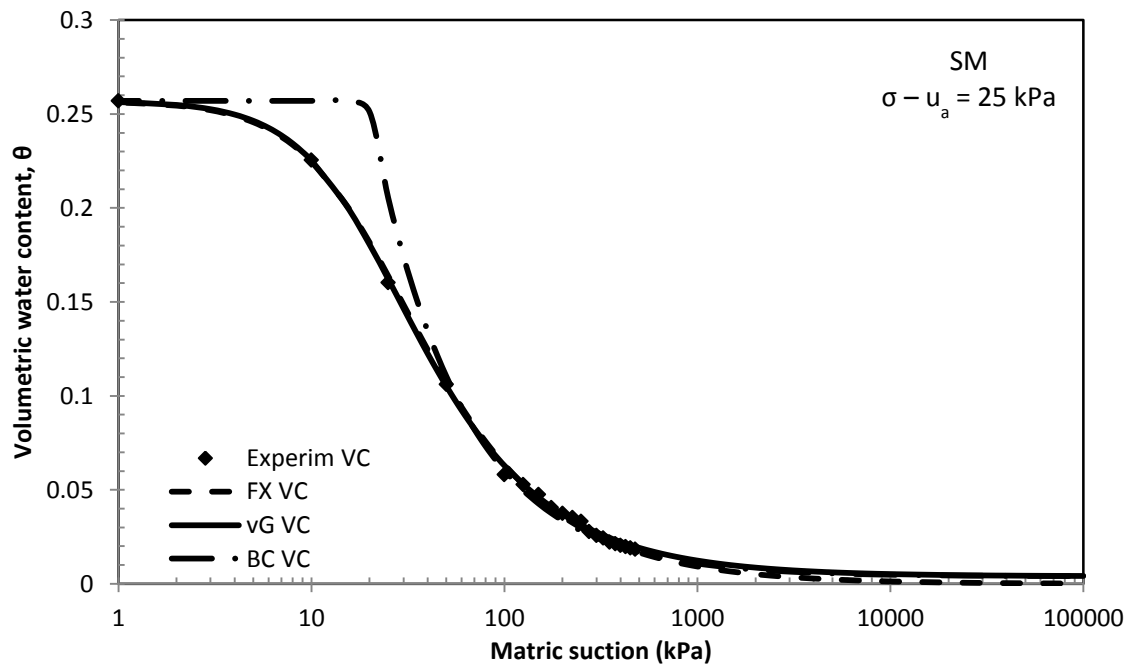
BC – Brooks and Corey model

SM – silty sand soil

SC – clayey sand soil

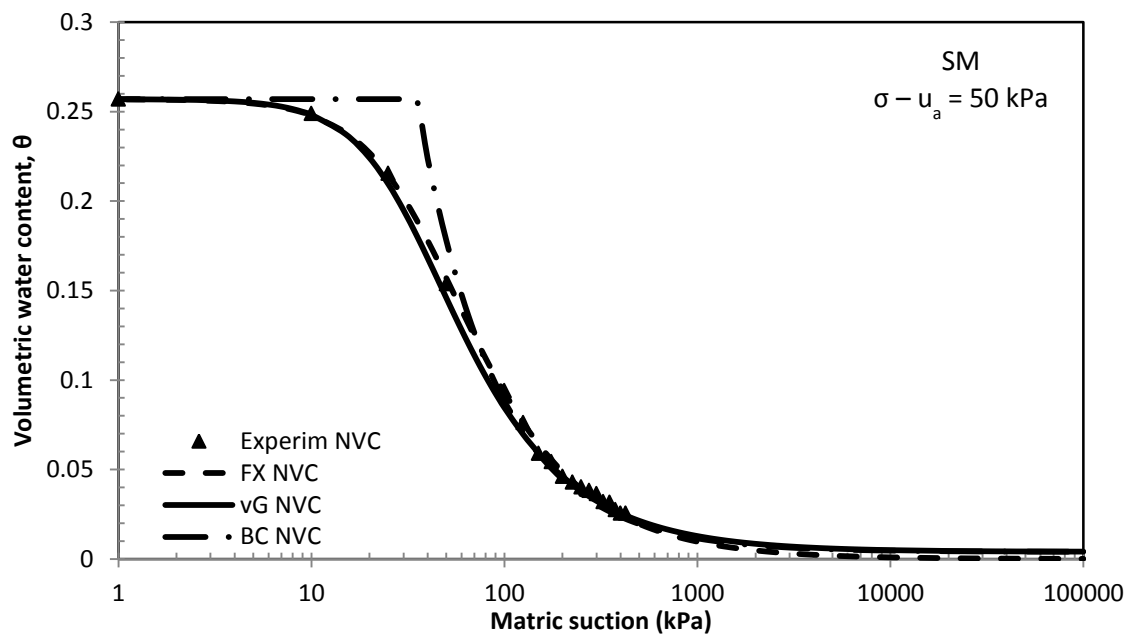


(a)

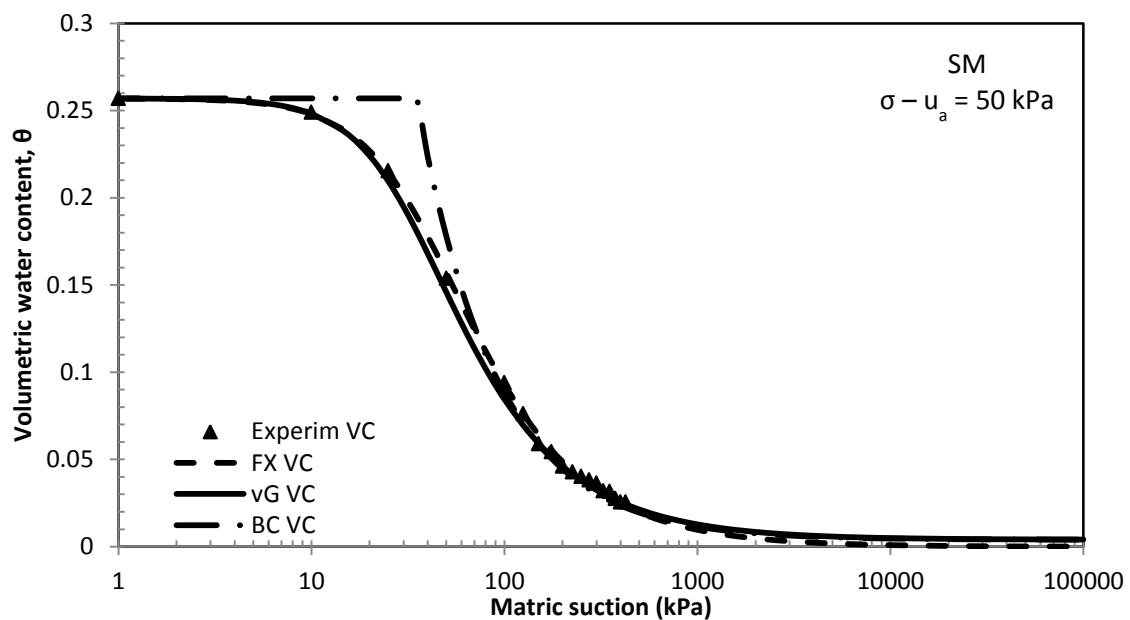


(b)

Figure 5.2 SWCCs modeled using the Fredlund and Xing, van Genuchten and Brooks and Corey equations for silty sand soil with a) NVC, and b) VC for $\sigma - u_a = 25 \text{ kPa}$

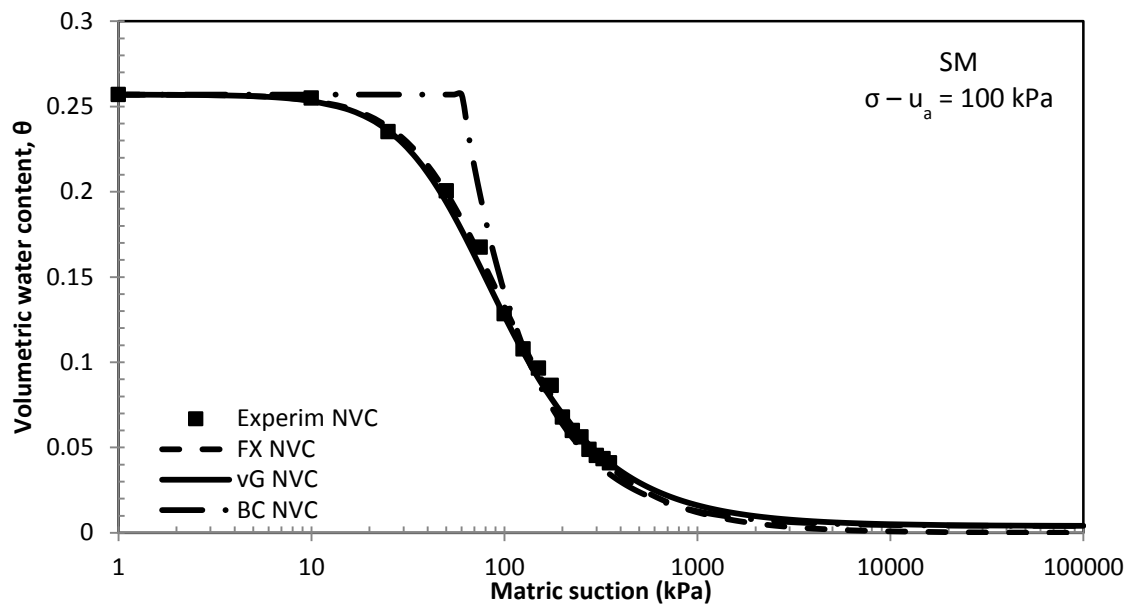


(a)

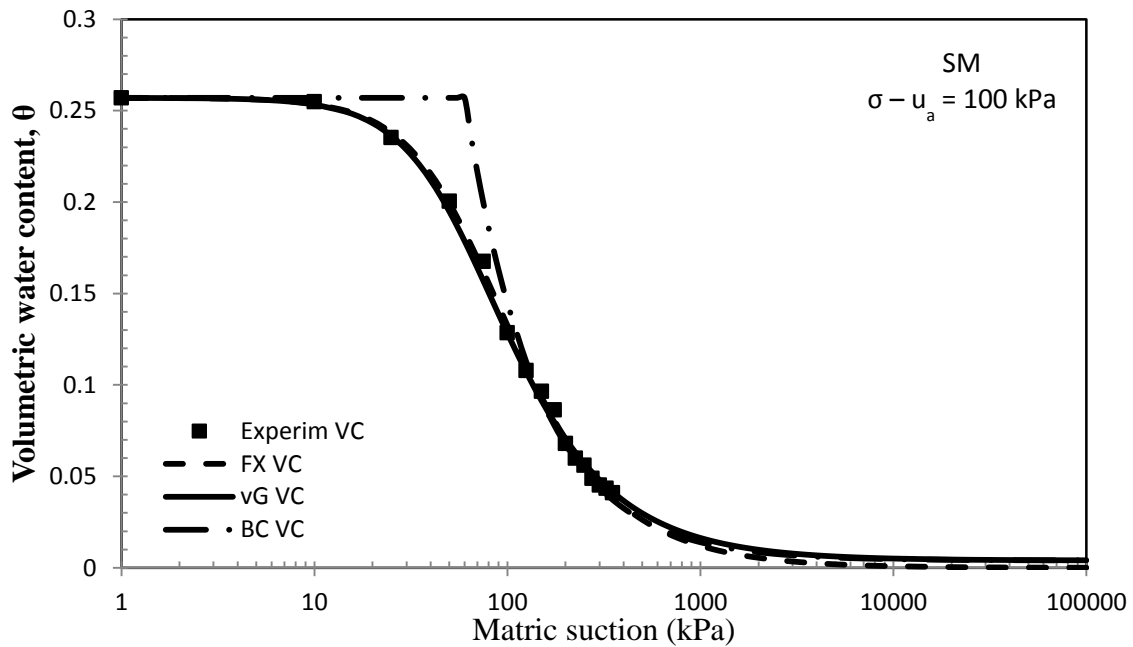


(b)

Figure 5.3 SWCCs modeled using the Fredlund and Xing, van Genuchten and Brooks and Corey equations for silty sand soil with a) NVC, and b) VC for $\sigma - u_a = 50$ kPa

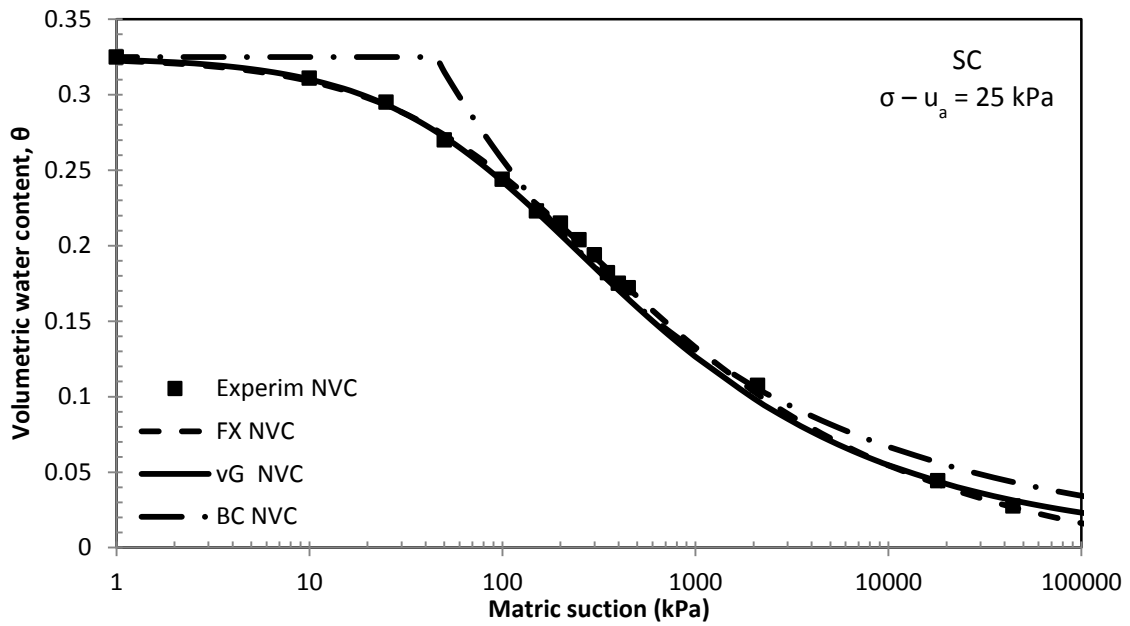


(a)

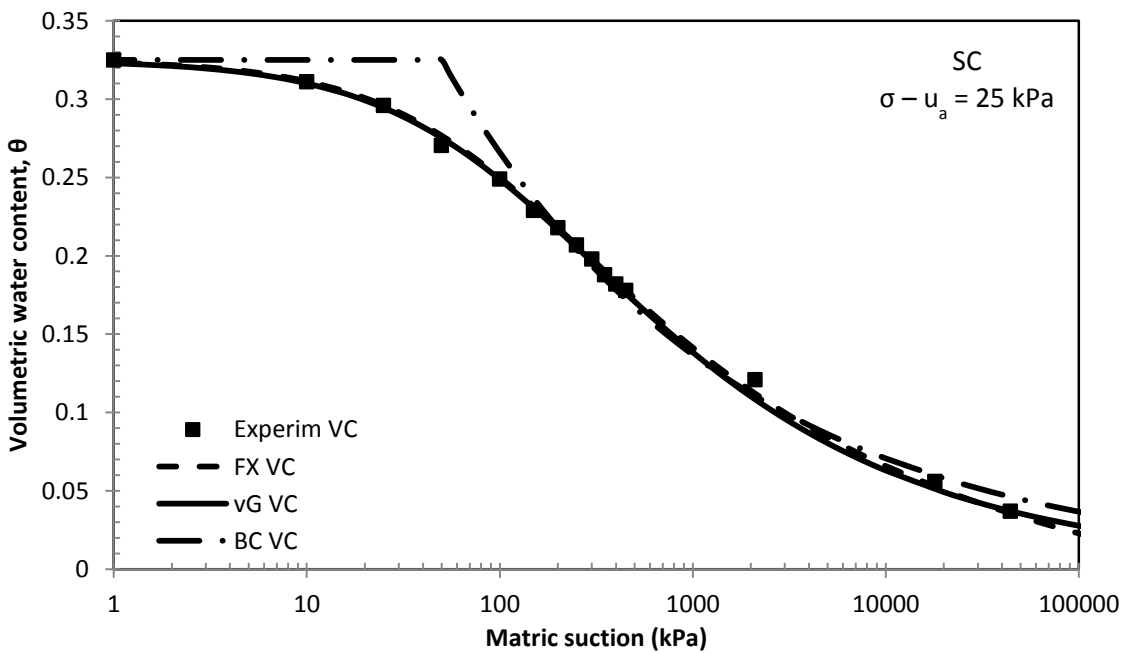


(b)

Figure 5.4 SWCCs modeled using the Fredlund and Xing, van Genuchten and Brooks and Corey equations for silty sand soil with a) NVC, and b) VC for $\sigma - u_a = 100$ kPa

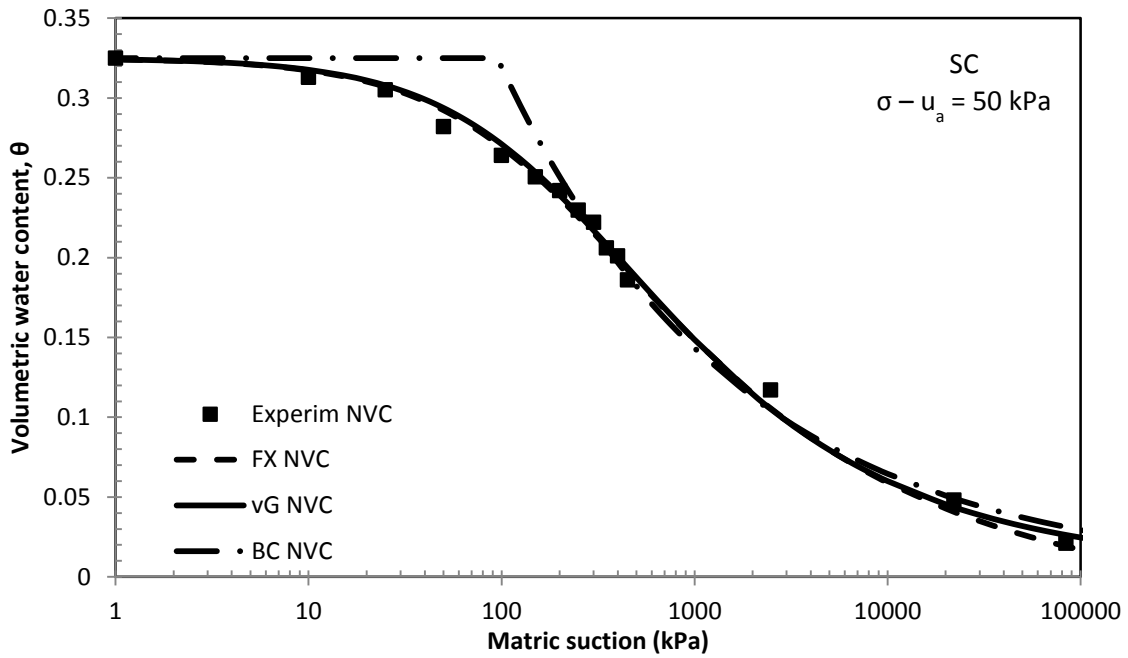


(a)

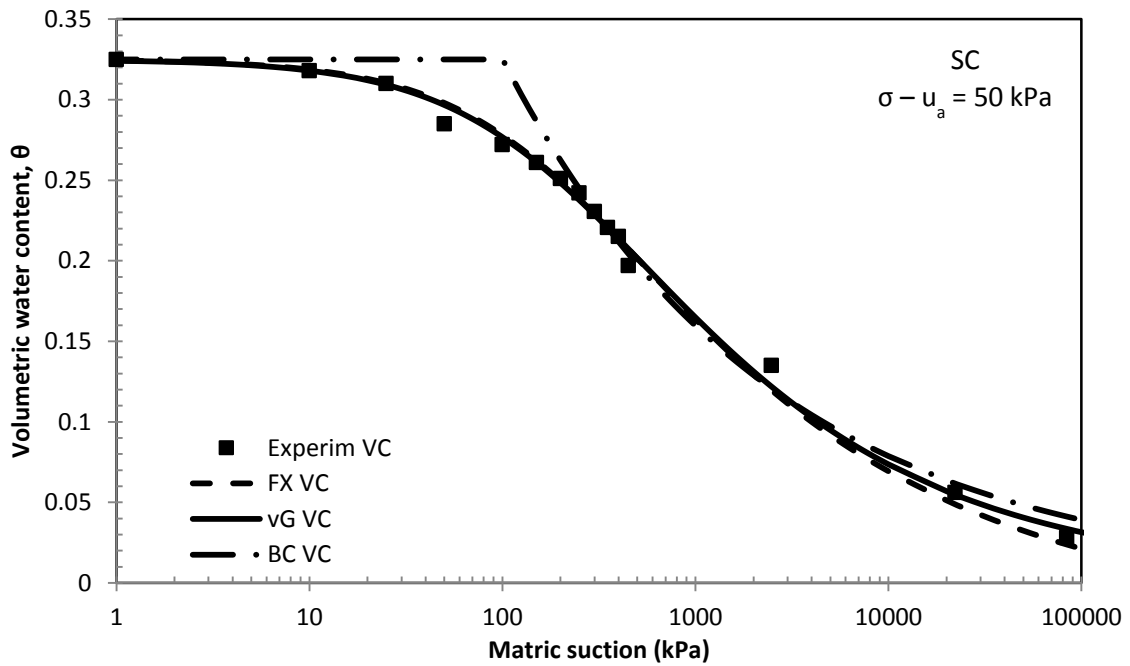


(b)

Figure 5.5 SWCCs modeled using the Fredlund and Xing, van Genuchten and Brooks and Corey equations for clayey sand soil with a) NVC, and b) VC for $\sigma - u_a = 25$ kPa

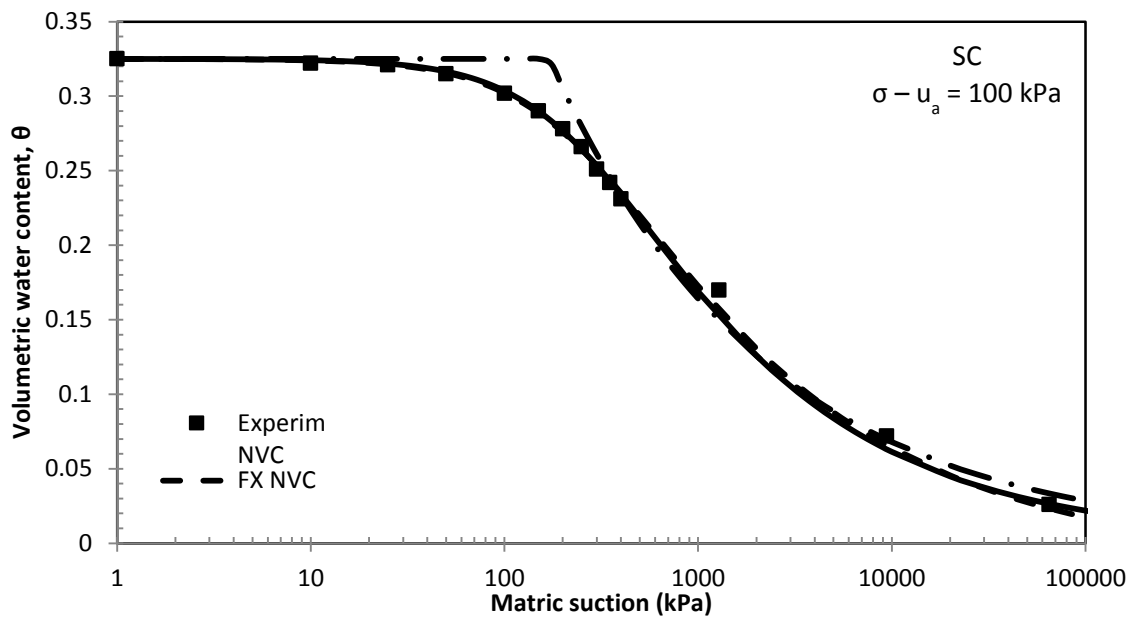


(a)

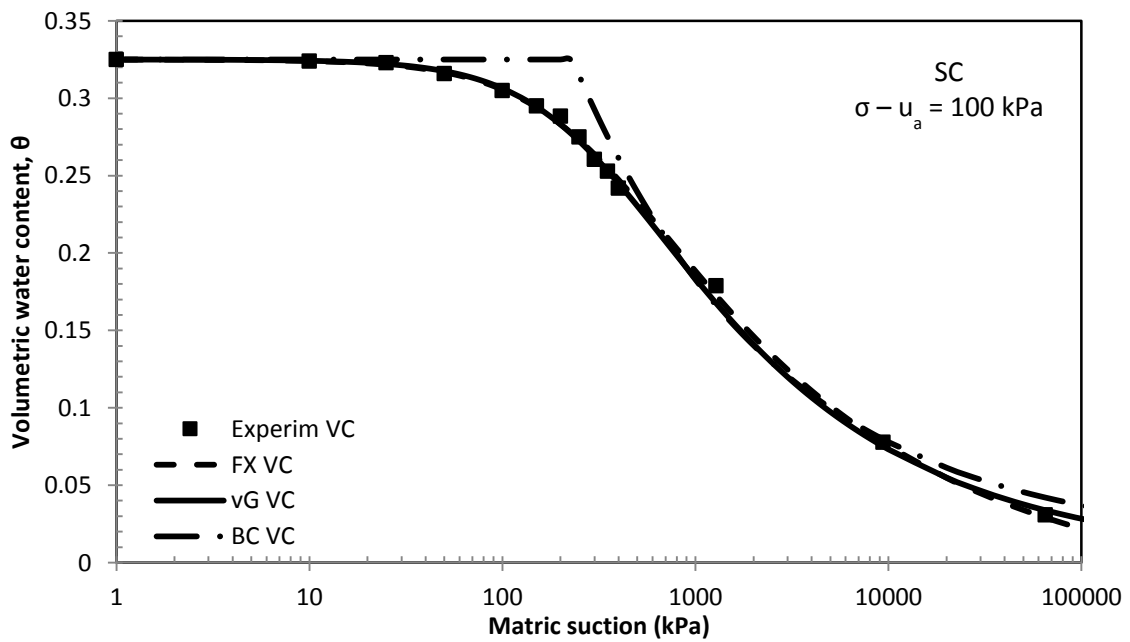


(b)

Figure 5.6 SWCCs modeled using the Fredlund and Xing, van Genuchten and Brooks and Corey equations for clayey sand soil with a) NVC, and b) VC for $\sigma - u_a = 50$ kPa



(a)



(b)

Figure 5.7 SWCCs modeled using the Fredlund and Xing, van Genuchten and Brooks and Corey equations for clayey sand soil with a) NVC, and b) VC for $\sigma - u_a = 100 \text{ kPa}$

As it can be clearly seen from the above plots, the Brooks and Corey (1964) model does not catch up all the experimental values over the entire suction range, whereas both van Genuchten (1980) and Fredlund and Xing (1994) models reasonably give a smoother fit for both test soils. Brooks and Corey model is proposed based on two parameters equation, the model is open form about the air-entry pressure and loses applicability at higher suctions approaching the residual water content (Lu and Likos, 2004).

Unlike the Brooks and Corey (1964) model, both van Genuchten (1980) and Fredlund and Xing (1994) models have three fitting parameters, α , n and m , which give a higher flexibility to the model equations and smoother fit to the experimental values, as seen in figure 5.7 (a) and (b) above. In these both model equations, α is related to the air-entry values having an inverse unit of pressure, n is related to the pore-size distribution of the soil and m parameter is related to the overall symmetry of the characteristic curve. In van Genuchten's (1980) equation, the m parameter is related to the n parameter by the equation $m = 1 - 1/n$ for simplicity, but Fredlund and Xing (1994) equation considers each parameter independently which gives the model a greater flexibility to fit well over a wider range of suction.

Based on modeling of the experiment data using van Genuchten's equation, the silty sand soil has higher values of all the three fitting parameter, α , n and m compared to the clayey sand soil under the same net normal stress. This gives a steeper slope at the air-entry values and a relatively gentle slope at higher suction values to the SWCC of the silty sand soil, resulting in lower air-entry values. The opposite is true for the clayey sand

soil. This pretty much relates with previous studies (Lu and Likos, 2004). Table 5.1 summarizes this statement by considering the SWCCs of both test soils under a net normal stress of 50 kPa with no volume change consideration.

Table 5.1 Summary of SWCC fitting parameters for silty sand and clayey sand soils under a net normal stress of 50 kPa with no volume change consideration

Curve Fitting Parameters				
Soil Type	van Genuchten (1980)		Fredlund and Xing (1994)	
Silty sand (SM)	α (1/kPa) =	0.031	a (1/kPa) =	40
	n =	2.15	n =	1.92
	m =	0.455	m =	0.53
	θ_s =	0.2578	θ_s =	0.2578
	θ_r =	0.0005	θ_r =	0.001
	ψ_b (kPa) =	27	ψ_b (kPa) =	28
Clayey sand (SC)	α (1/kPa) =	0.00486	a (1/kPa) =	180
	n =	0.98	n =	0.98
	m =	0.46	m =	0.421
	θ_s =	0.3249	θ_s =	0.3249
	θ_r =	0.005	θ_r =	0.003
	ψ_b (kPa) =	70	ψ_b (kPa) =	70

5.4 Effect of Volume Change on SWCCs

The effect of volume change has generally been ignored by most researchers during construction of SWCC due to the relatively small change in volume during soil-water characteristic tests. Ng et al. (2000) observed no effect on the general trend of soil-water characteristic curves (SWCCs) with and without considering volume change for sandy silt/clay using volumetric pressure plate tests. This is generally true for coarser soils which undergo a very small change in volume over the entire range of suction states during the SWCC test, as it was observed for the silty sand soil in this study. However, it is not necessarily true for fine-grained soils which undergo relatively higher volume change during the entire stay under the test. This was also clearly observed under this study for the clayey sand soil, as shown in the figures 5.8 through 5.13. The SWCCs were fitted using the Fredlund and Xing (1994) model for both test soils.

As it can be readily observed from these plots, there is no change in SWCCs of the silty sand soil under various net normal stresses due to change in volume of the test specimen, hence the effect of volume change on SWCCs of coarse-grained soils can be ignored without incorporating significant error into the test results and measurements, and the corresponding SWCCs.

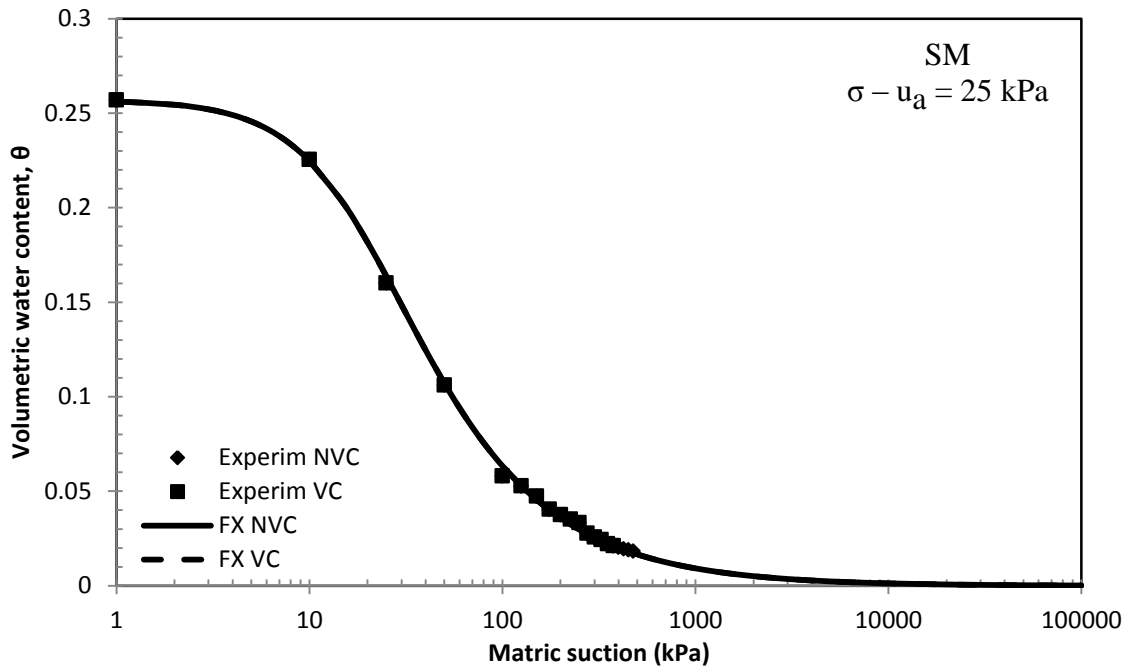


Figure 5.8 SWCCs of silty sand soil fitted using the Fredlund and Xing model with both volume change and no volume change consideration for net normal stress of 25 kPa

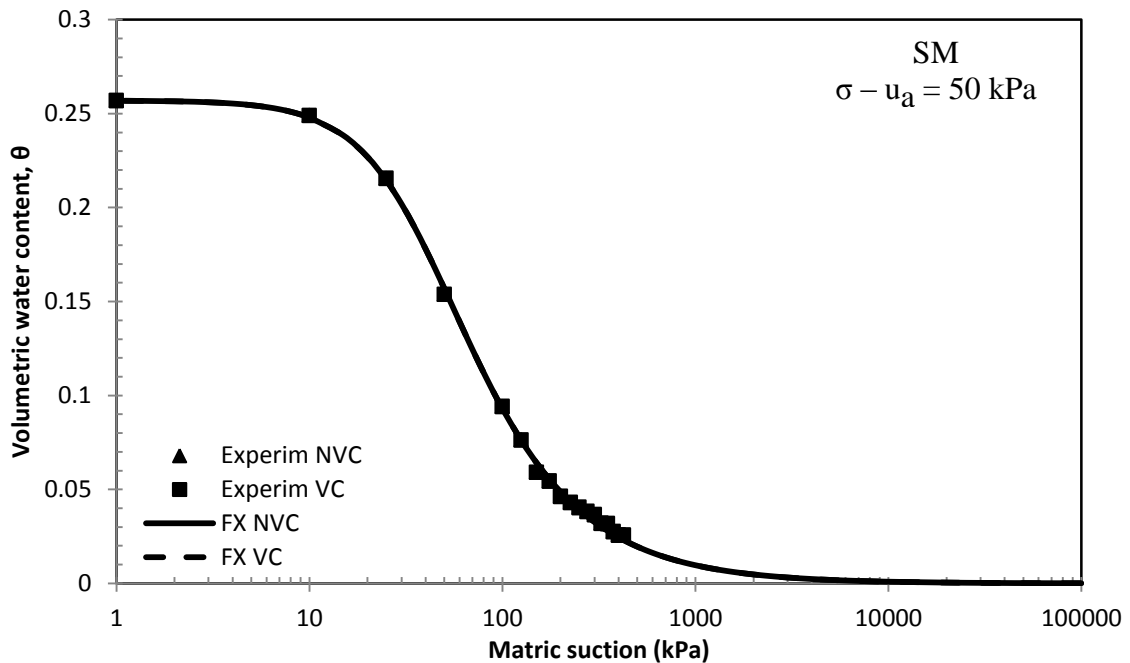


Figure 5.9 SWCCs of silty sand soil fitted using the Fredlund and Xing model with both volume change and no volume change consideration for net normal stress of 50 kPa

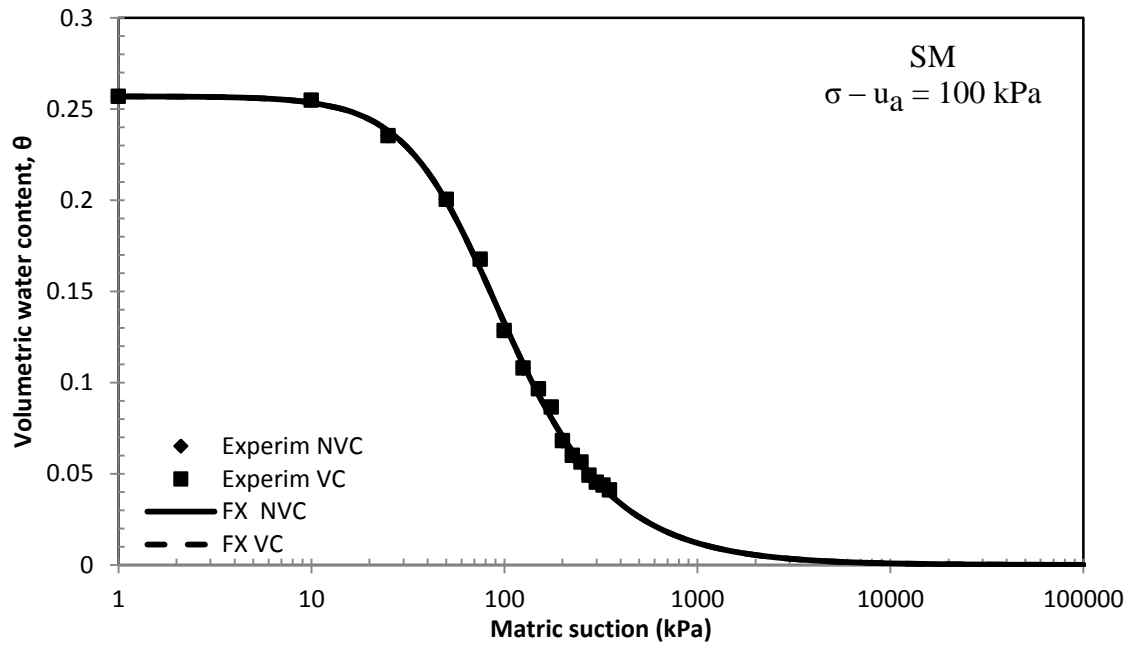


Figure 5.10 SWCCs of silty sand soil fitted using the Fredlund and Xing model with both volume change and no volume change consideration for net normal stress of 100 kPa

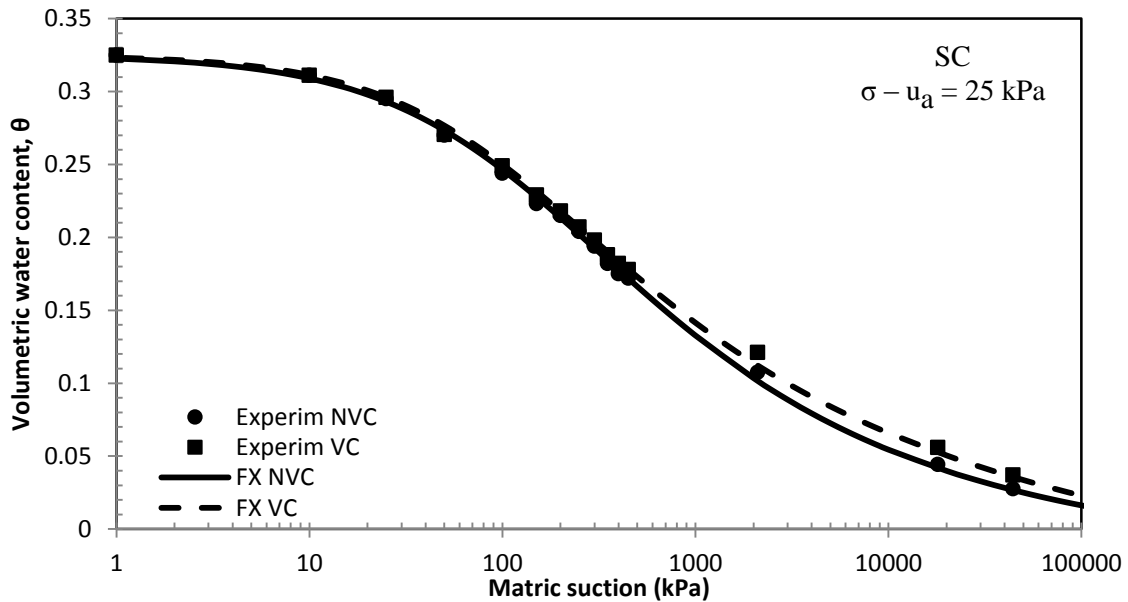


Figure 5.11 SWCCs of clayey sand soil fitted using the Fredlund and Xing model with both volume change and no volume change consideration for net normal stress of 100 kPa

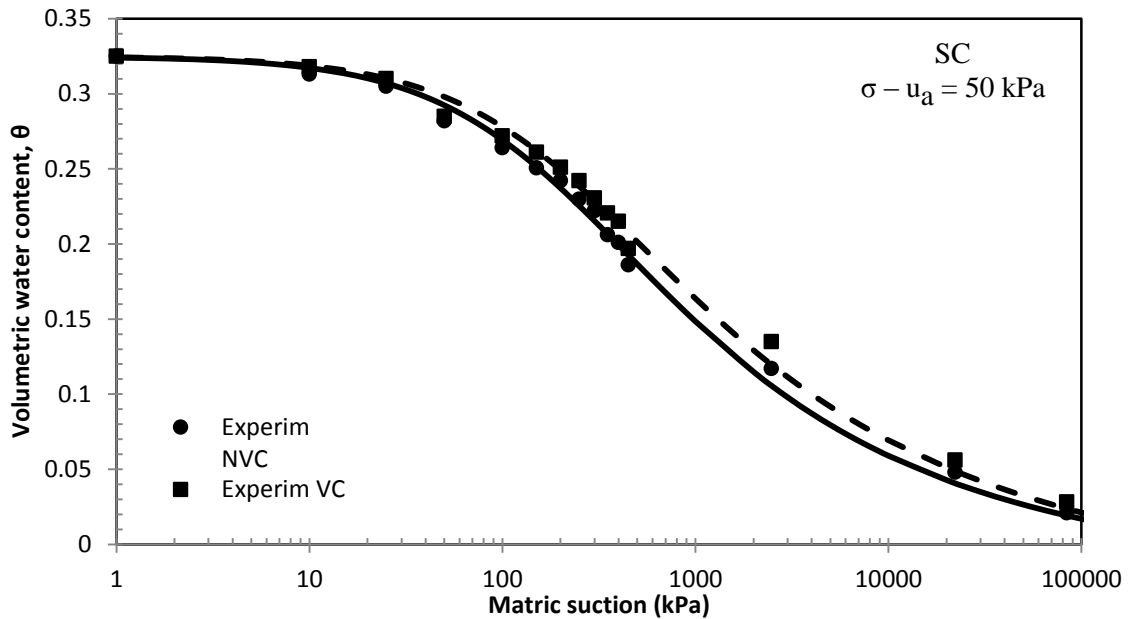


Figure 5.12 SWCCs of clayey sand soil fitted using the Fredlund and Xing model with both volume change and no volume change consideration for net normal stress of 50 kPa

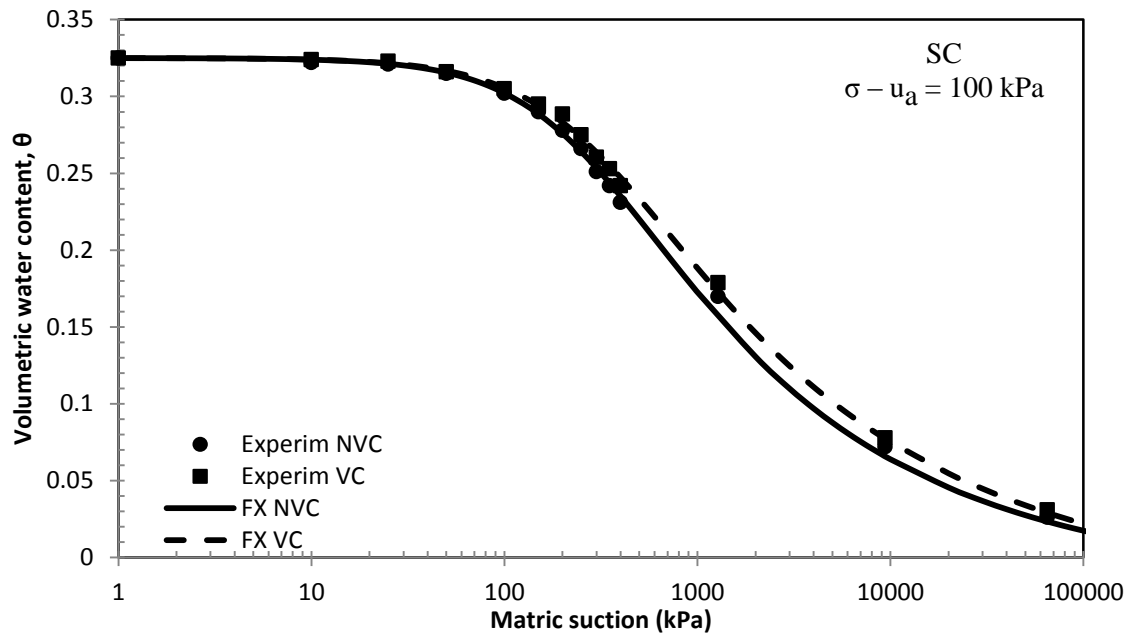


Figure 5.13 SWCCs of clayey sand soil fitted using the Fredlund and Xing model with both volume change and no volume change consideration for net normal stress of 100 kPa

As it can be clearly seen from the above plots, there is a more considerable effect of volume change on the SWCCs of the clayey sand soil under various net normal stresses. Considering the effect of volume change, the SWCC construction shifted towards the right for all net normal stresses, resulting in an increase in the air-entry values and the residual water content of the soil. In addition to this, the slope of the SWCC with no volume change consideration is relatively steeper than the one with volume change considered. This also overestimates the desaturation rate of the soil. Hence, neglecting the effect of volume change on SWCCs of clayey sand soils underestimates the air-entry value and overestimates the desaturation rate of the soil, thus inducing a cumulative error in reporting the SWCC model parameters of the soil.

5.5 Effect of Change in Net Normal Stress on SWCCs

Since the effect of volume change is very minimal on the SWCC of silty sand soil, only SWCCs with no volume change are presented here to see the effect of increase in net normal stress on the SWCCs. Based on Fredlund and Xing (1994) model for the silty sand soil, at 25kPa the air-entry value is 20 kPa, and the value increases to 68 kPa at a net normal stress of 100 kPa. As the net normal stress increases, the SWCC of the silty sand soil shifted to the right, resulting in an increase in the air-entry value of the soil. This entails that a higher suction is required to drain the same amount of water from the soil at a higher net normal stress than at a lower net normal stress. In other words, it requires a higher suction to dry soils at deeper depths undergoing higher overburden pressure than the same soils at shallow depths.

The fitting parameters “ α ” and “ a ” related to the air-entry value of the soils for van Genuchten and Fredlund and Xing models, respectively, have also indicated some trend which supports the increase in the air-entry value as the net normal stress increases. From van Genuchten (1980) model, the α parameter slightly decreases with the increase in net normal stress, and from Fredlund and Xing (1994) modeling, the a parameter increased with an increase in net normal stress, thereby increasing the air-entry value in both cases. Table 5.1 shows the effect of increase in net normal stress on the fitting parameters of the both test soils.

In addition to this, the slope of the SWCCs for the clayey sand soil gets gentler as the net normal stress increases. This has been observed by a slight decrease in both the m and n parameters as the net normal stress increases. This implies that the pores of

relatively fine-grained soils drains faster at lower net normal stress than at higher net normal stress. On the contrary, the slope of the SWCCs for the clayey sand soil gets steeper as the net normal stress increase. This has been observed by slight increase in both the m and n parameters as the net normal stress increases. This implies that the pores of coarse-grained soils drains faster at higher net normal stress than at lower net normal stress.

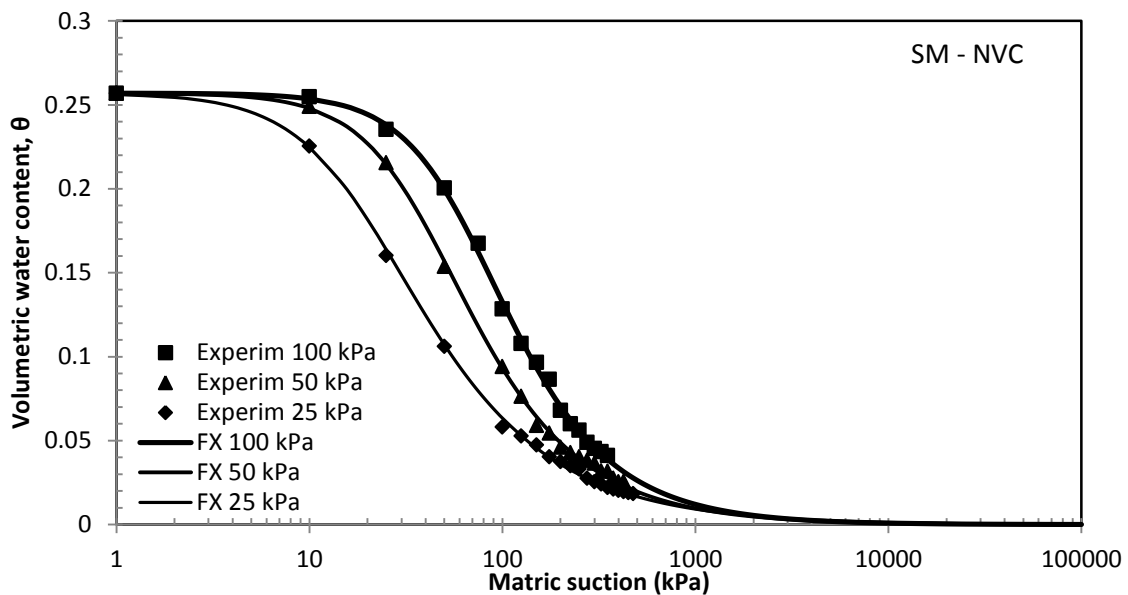
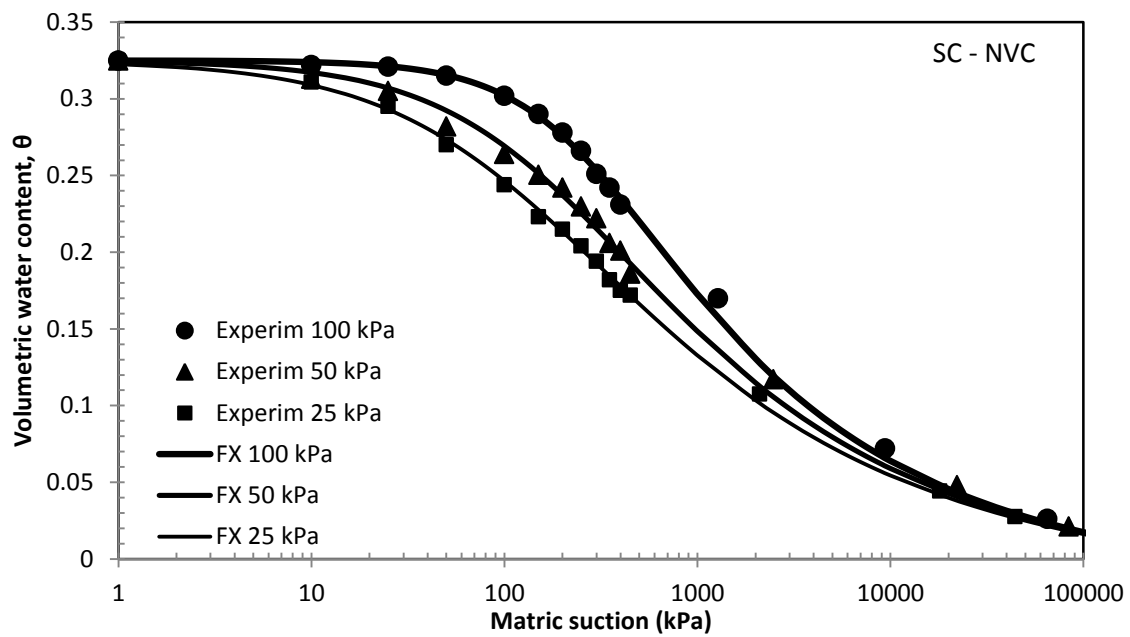


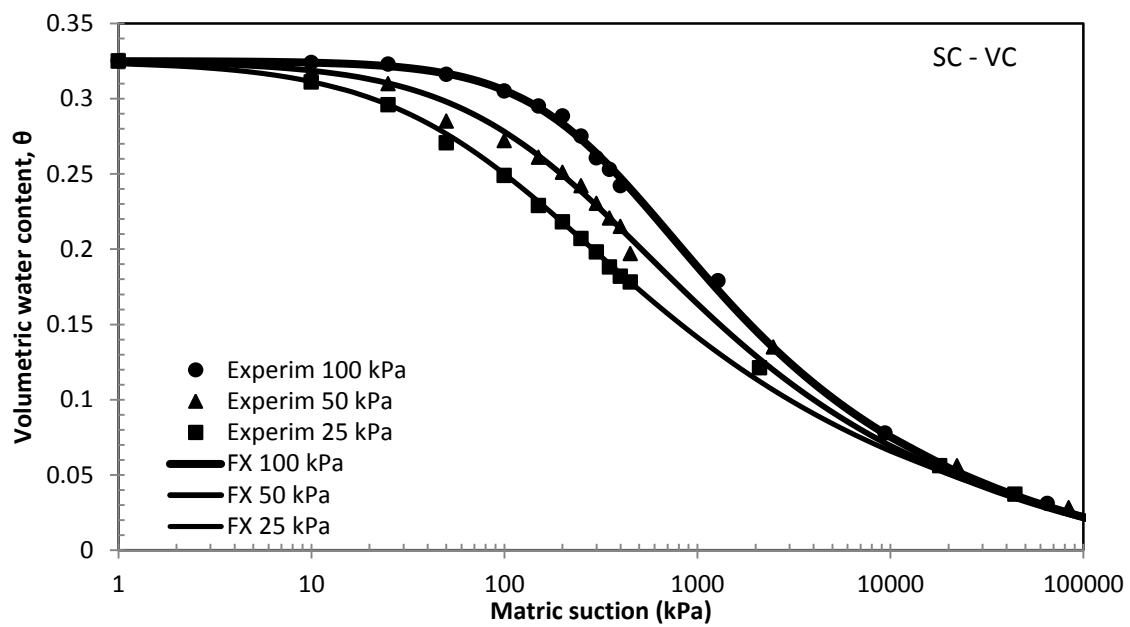
Figure 5.14 Effect of net normal stress on SWCCs of silty sand soil fitted using the Fredlund and Xing model for no volume change case

For the clayey sand soil, SWCC with both volume change and no volume change cases are considered to see the effect of an increase in net normal stress on SWCCs. The general trend of the SWCCs follows the same fashion as those of silty sand soil for both cases, as seen in figure 5.15 below. As the net normal stress increases, the SWCC of the clayey sand soil shifts to the right, resulting in an increase in the air-entry value of the

soil. Based on the Fredlund and Xing (1994) model for the clayey sand soil, at net normal stress of 25 kPa, with NVC consideration, the air-entry value of the soil is 25 kPa. For the same case at 50 kPa net normal stress, the air-entry value of the soil is 70 kPa, and the value increases to 100 KPa at highest net normal stress of 100 KPa. As the net normal increases, the SWCC of the clayey sand soil also shifts to the right, resulting in increase in air-entry value of the soil. This entails that a higher suction is required to drain the same amount of water from the soil at a higher net normal stress due to the smaller pore distribution of the soil. The same tendency, a shift to the right of the SWCCs with an increase in net normal stress, was observed for clayey sand soil also for both volume change and no volume change consideration.



(a)



(b)

Figure 5.15 Effect of net normal stress on SWCCs of clayey sand soil fitted using the Fredlund and Xing model with a) no volume change and b) volume change consideration

5.6 Effect of pore-size distribution on SWCCs

It is well known that the general behavior of the soil-water characteristic curves is dependent on the soil type, as shown in figures 5.16 through 5.18 below for this particular study for intermediate sandy soils. Results from this study have shown that soils with larger particles have low specific surface area and hence have the lowest capacity for water absorption within a short range of suction. On the contrary, soils with smaller particles have higher specific surface area and hence have the highest water absorption capacity within a wider range of suction values.

It is clearly observed that the clayey sand soil has higher air-entry value than the silty sand soil for any given net normal stress induced on the soil. Therefore, as expected, higher pore-air pressures, using axis translation technique, are required to drain the same amount of water from fine-grained soils than from coarse-grained soils. The slope of the SWCCs for silty sand soil is higher than the clayey sand soil over the same suction range. Pores of Coarse-grained soils drain much faster than fine pores of fine-grained soils under the same suction range. The following figures further substantiate the effect of particle-size distribution on the soil-water retention properties of both silty sand and clayey sand soils.

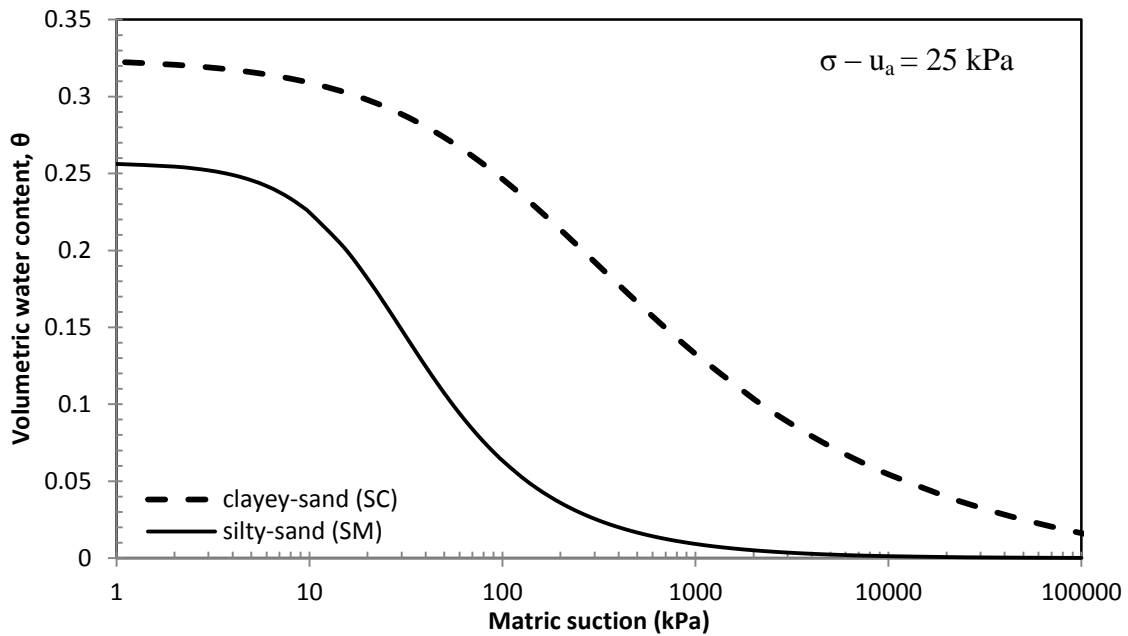


Figure 5.16 Effect of pore-size distribution on SWCCs of SC and SM soils modeled using the Fredlund and Xing (1994) equation with NVC consideration for $\sigma - u_a = 25$ kPa

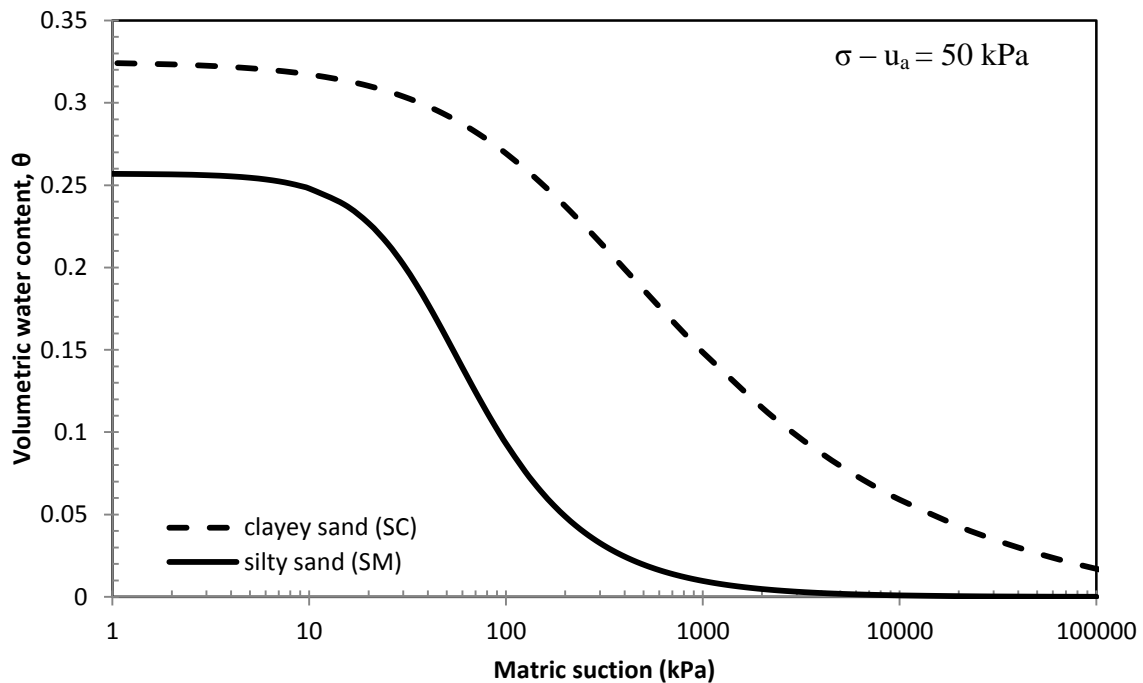


Figure 5.17 Effect of pore-size distribution on SWCCs of SC and SM soils modeled using the Fredlund and Xing (1994) equation with NVC consideration for $\sigma - u_a = 50$ kPa

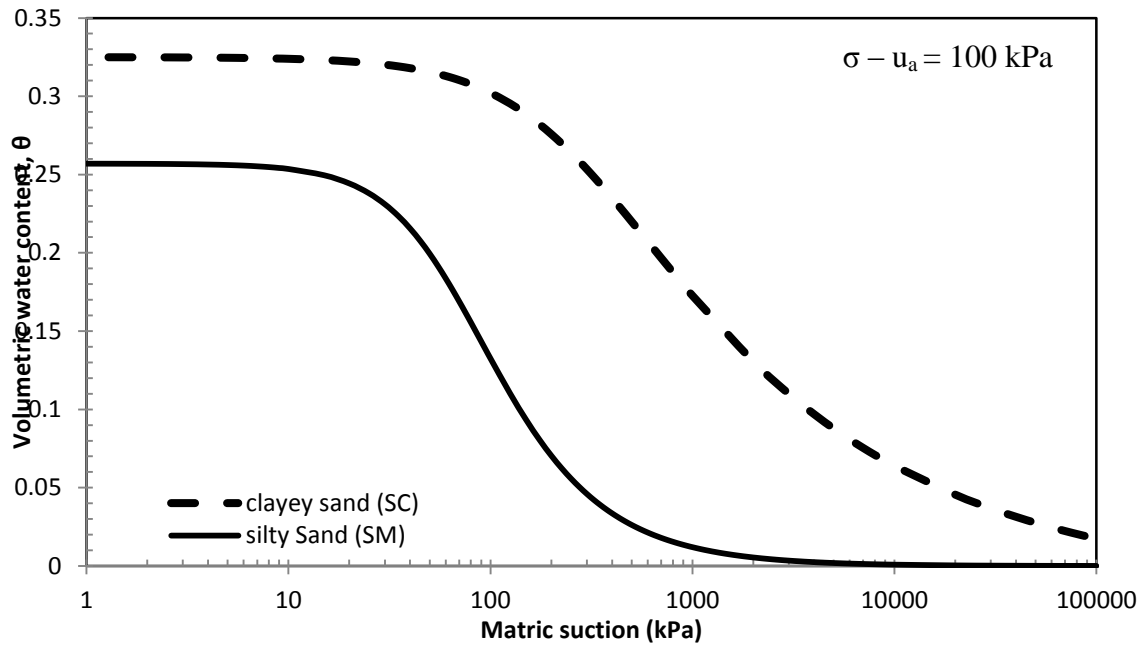


Figure 5.18 Effect of pore-size distribution on SWCCs of SC and SM soils modeled using the Fredlund and Xing (1994) equation with NVC consideration for $\sigma - u_a = 100$ kPa

5.7 Prediction of Stress/volume-controlled SWCCs for Wider Range of Net Normal Stresses

In the absence of sufficient test results or with limited experimental data, predicting the soil-water characteristic parameters of a given soil based on the existing experimental data set has a vital merit in engineering practice. Even experienced engineers use this predicted data for design purposes by carefully analyzing and processing the observed experimental data sets obtained from a carefully designed and conducted test. Taking this into consideration, a prediction of the SWCCs was made for a wide range of net normal stress states for both test soils in order to assess the effect of a significant increase in net normal stress on the SWCCs for both test soils. No volume

change case was considered for either test soil and the trends obtained were found to be pretty consistent with the trends observed from the experimental results.

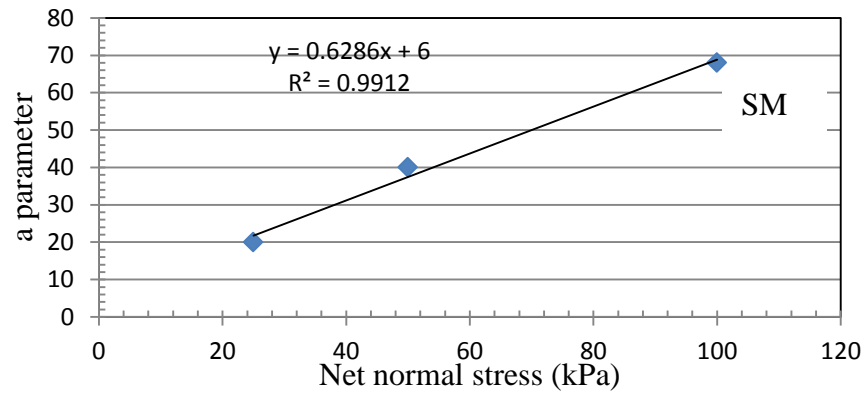
A summary of the model parameters used in all the three modeling equations, as well as the procedures followed to predict these model parameters for a selected range of hypothetical net normal stresses, are included below.

Table 5.2 Summary of SWCC fitting parameters for silty sand and clayey sand soils fitted using three model equations under net normal stress of 25, 50 and 100 kPa

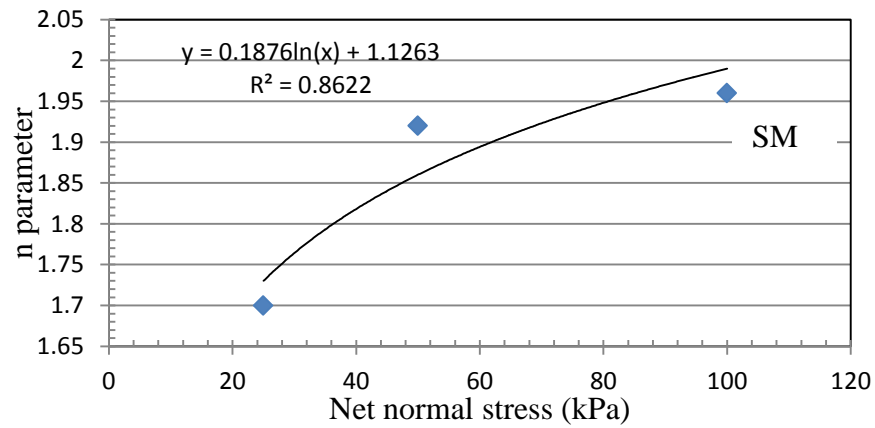
Model	Curve fitting parameters	Silty sand (SM) soil with NVC			Clayey sand (SC) soil with NVC			Clayey sand (SC) soil with VC		
		$\sigma - u_a$ (kPa)			$\sigma - u_a$ (kPa)			$\sigma - u_a$ (kPa)		
		25	50	100	25	50	100	25	50	100
FX (1994)	a	20	40	68	130	180	260	91	210	300
	n	1.7	1.92	1.96	0.85	0.98	1.4	0.93	0.98	1.35
	m	0.5	0.53	0.58	0.47	0.421	0.31	0.355	0.395	0.3
	ψ_b (kPa)	10	18	31	25	70	100	32	52	103
vG (1980)	α (1/kPa)	0.053	0.031	0.017	0.0105	0.0049	0.0038	0.0088	0.0047	0.0035
	n	1.789	2.15	2	0.94	0.98	1.465	0.875	0.95	1.43
	m	0.48	0.455	0.538	0.41	0.46	0.315	0.42	0.41	0.295
	ψ_b (kPa)	10	15	29	28	70	100	32	52	103
BC (1964)	λ	0.87	1.05	1.2	0.295	0.35	0.387	0.29	0.31	0.41
	ψ_b (kPa)	20	35	60	45	95	115	50	100	122

By closer observation of all Fredlund and Xing (1994) model parameters, the best fitting equation was established for all basic model parameters with respect to a particular value of net normal stress used to conduct the experiment. These best-fitting model parameters were then used to project SWCC data forward to predict the theoretical SWCCs of the two test soils for various net normal stresses that were not considered in the experimental program. The plots of the model parameters with respect to the net normal stress with their respective fitting equation are presented in figures 5.19 and 5.20 below.

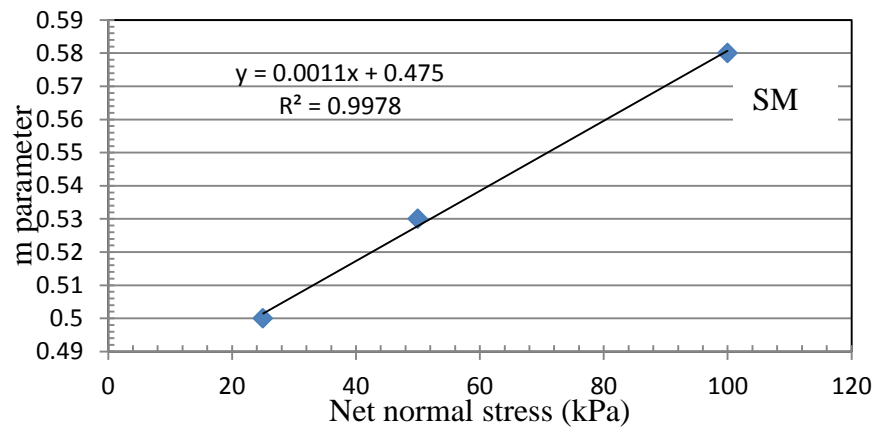
As it can be readily seen from these graphs, all the model parameters except the n parameter for silty sand soil, were able to fit a linear trend with respect to net normal stress. The n parameter for the silty sand soil was best fitted with natural logarithmic equation as shown below. All the model parameters, but the m parameter for the clayey sand soil, followed the same trend that is; they increase with an increase in net normal stress regardless of their values. The m parameter for the clayey sand soil slightly decreased with increase in net normal stress, while it is increased linearly with an increase in net normal stress for the silty sand soil. This makes the slope of the clayey sand soil gentler as the net normal stress increases. This implies that much higher suction is required to desaturate relatively the fine-grained clayey sand soil compared to the poorly graded silty sand soil at a higher net normal stresses. Soils with larger pore-size distribution, desaturates at faster rate as compared to soils with smaller pore-sizes because it takes less pore-air pressure to desaturate larger pores filled with water than smaller pores. This substantiates similar observations reported in all previous sections.



(a)

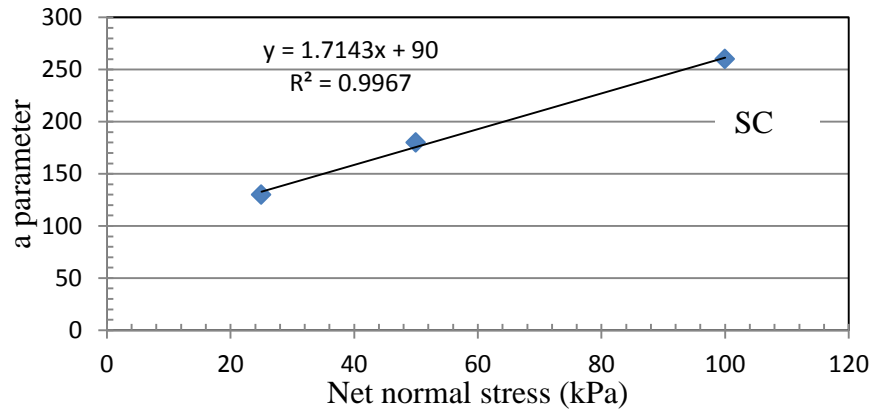


(b)

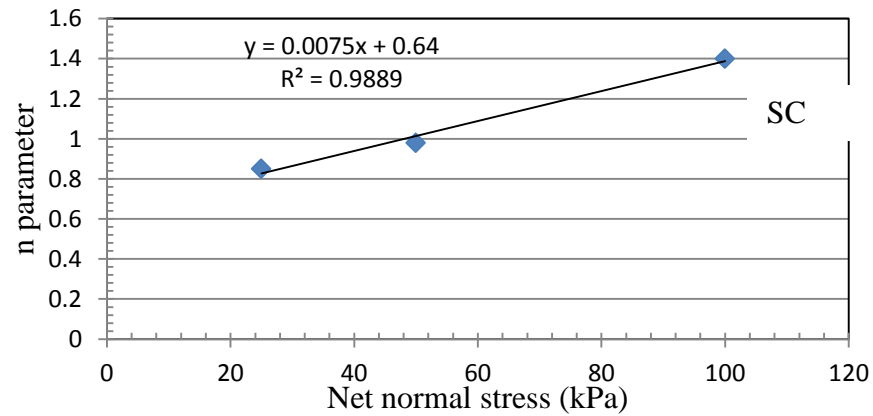


(c)

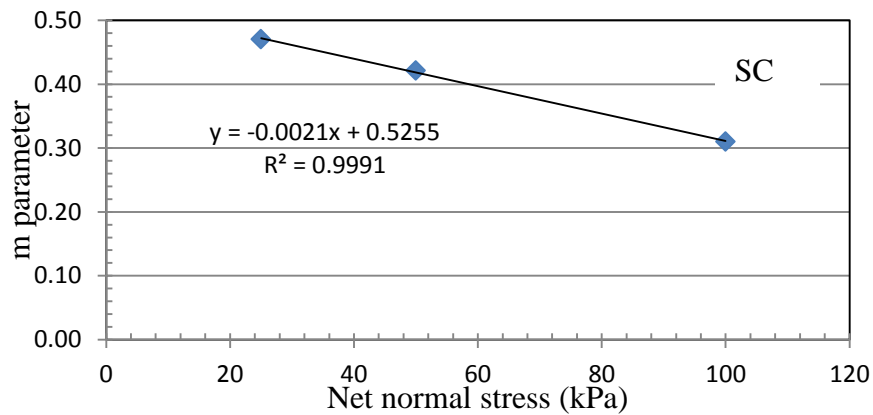
Figure 5.19 Variation of Fredlund and Xing model parameters with respect to net normal stress for SM soil with no volume change consideration for (a) a parameter, (b) n parameter, and (c) m parameter



(a)



(b)

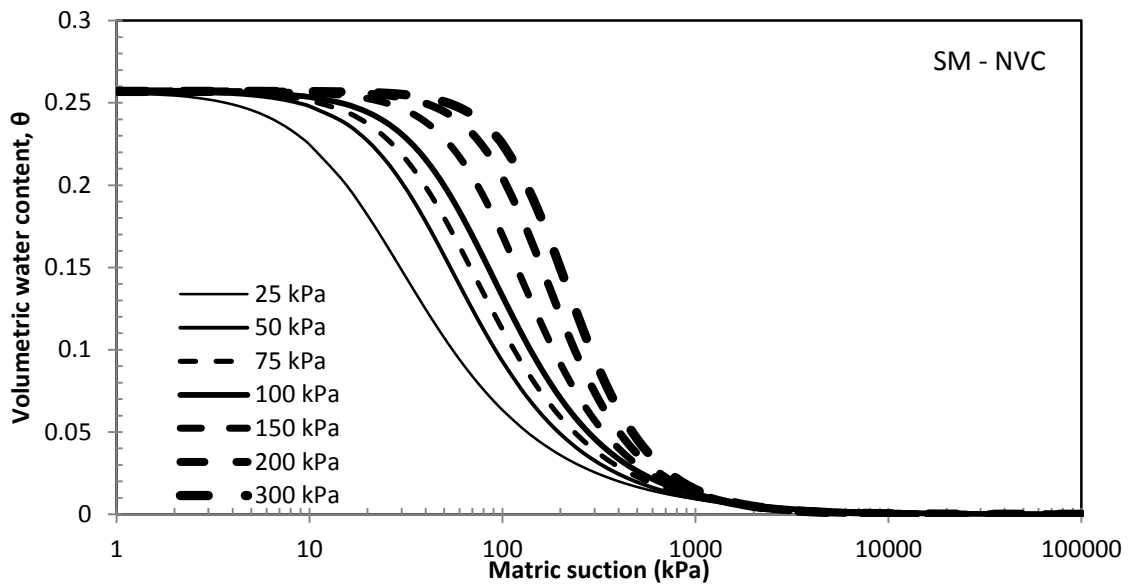


(c)

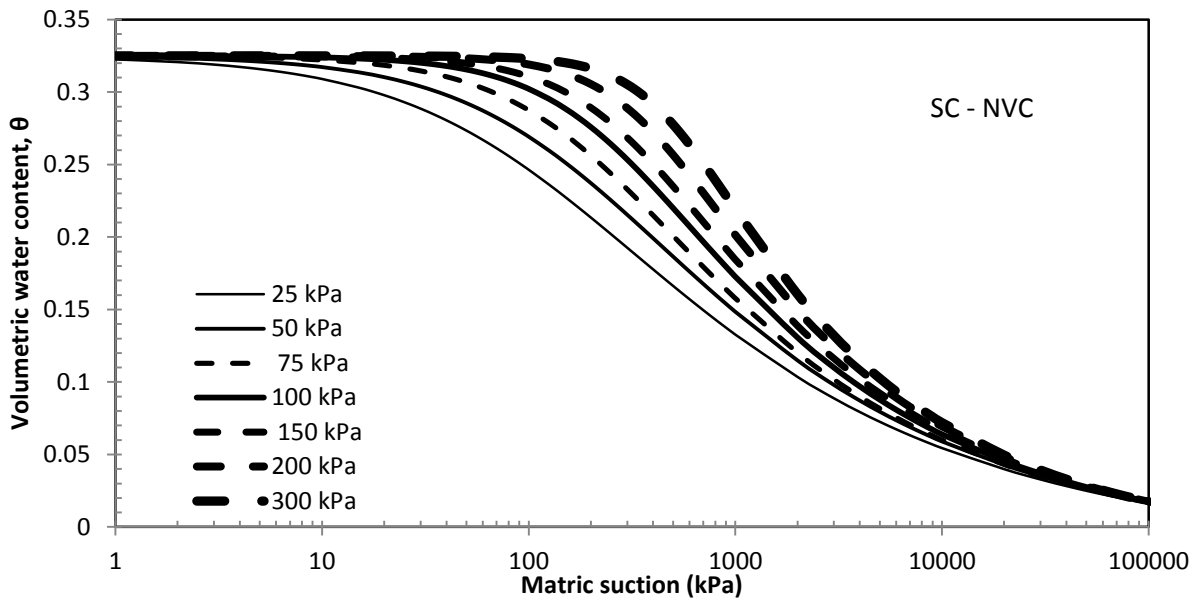
Figure 5.20 Plot of Fredlund and Xing model parameters with respect to net normal stress for clayey sand soil with no volume change consideration for (a) a parameter, (b) n parameter, and (c) m parameter

Unlike the silty sand soil, the m parameter of the clay-sand soil does not show much change as the net normal stress increases. This indicates that the effect of an increase in net normal on the overall symmetry of the SWCC decreases at a higher net normal stress states than at a lower net normal stress states. The slight decrease in the m parameter is can be attributed to the presence of finer clay particles in the clayey sand soil, compared to the silty sand soil, which makes it more difficult to desaturate fine-grained soils at a higher net confinement pressure.

Based on the best fitted model parameters, the theoretical predictions of SWCCs for a wider range of net vertical stresses, other than the experimental stress values used in this work, was made to assess the effect of a significant increase in net normal stress on the SWCCs for both test soils. Theoretical SWCCs for net normal stresses of 25, 50, 75, 100, 150, 200 and 300 kPa were plotted using the Fredlund and Xing model for both test soils with no volume change (NVC) consideration, and are presented in figure 5.21 below. The SWCCs with the solid lines correspond to for the experimental net normal stresses considered in this work, and those with the dashed lines are for other hypothetical net normal stress states.



(a)



(b)

Figure 5.21 Theoretical SWCCs modeled using the Fredlund and Xing (1994) equation for a wider range of net normal stresses with NVC consideration for (a) SM soil, sand (b)

SC soil

The slope of the SWCCs for the silty sand soil gets steeper than the slope of the SWCCs for the clayey sand soil as net normal stress increases. This is further indication that the pores of coarse-grained soils still desaturates faster at a higher confinement compared to fine-grained soils. Again, comparing figure 5.21(a) and (b) above, and looking at the theoretical SWCCs of the two soils, the change in the air-entry value for the clayey sand soil is much higher than the silty sand soil for the same suction intervals. This further supports the fact that much higher suction is required to desaturate relatively fine-grained soil than the poorly graded silty sand soil at a higher net normal stress. The following table indicates a summary of all fitting parameters for both test soils modeled using the Fredlund and Xing (1994) equation for the experimental net normal stresses.

Table 5.3 Summary of FX SWCC fitting parameters for silty sand clayey sand soils fitted under a net normal stress of 25, 50 and 100 kPa with no volume change (NVC) consideration used to predict hypothetical SWCCs

		FX Model Parameters					
$\sigma - u_a$ (kPa)	Silty sand (SM) soil with NVC			Clayey sand (SC) soil with NVC			
	a	n	m	a	n	m	
25	20	1.7	0.5	130	0.85	0.47	
50	40	1.92	0.53	180	0.98	0.421	
100	68	1.96	0.58	260	1.4	0.31	

CONCLUSION AND RECOMMENDATIONS

6.1 Conclusions

The following summarizes the main conclusions derived from the present thesis work:

1. No change in the nature of the SWCCs for the silty sand soil was observed due to change in volume under all three net normal stresses applied on the test specimens tested. Hence, the effect of volume change on SWCCs of coarse-grained soils can be neglected without incorporating significant error in the assessment of both the air-entry value and the desaturation rate of the soils.
2. However, a noticeable shift to the right in the SWCCs of the clayey sand soil was observed when the change in volume considered in the calculation of volumetric water content. This yielded higher air-entry value and lower desaturation rate when compared with no volume change assumption. Therefore, neglecting the effect of volume change on fine-grained soils may underestimate the air-entry value and overestimate the desaturation rate of the soil.
3. As the net normal increases, the SWCCs of both soils shifted to the right, resulting in an increase in the air-entry value of the soils. A higher suction thereby, is required to drain the same amount of water from the soil at a higher net normal stress than at a lower net normal stress. In other words, it requires a higher suction to dry soils at larger depths than the same soils at shallow depths.
4. By constructing theoretical SWCCs for both test soils for a wider range of net normal stresses from the projected model parameters, it was observed that at a relatively high confinement pressure the effect of an increase in net normal stress has

little effect on the slopes of the SWCCs. Hence, at a higher confinement pressure the desaturation rate of both soils does not change considerably. Again, comparing the theoretical SWCCs of the two test soils, the change in the air-entry value of the clayey sand soil is greater at a higher suction value than the change in the air-entry value of the silty sand soil at the same suction range. This implies that a higher suction increase (pore-air pressure) is required to remove a small quantity of water from a relatively fine-grained soil than it is required for a coarse-grained soil at a higher net normal stresses. Soils with larger pore-size distribution desaturates at faster rate as compared to soils with smaller pore-sizes as it takes less pore-air pressure to desaturate the larger pores filled with water than the smaller pores.

5. All the Fredlund and Xing (1994) model parameters, except the n parameter follows a linear trend with respect to the net normal stress for both test soils for this thesis work.

6.2 Recommendations

Based on this study, the following recommendations are made for future studies:

1. Under this investigation, the soil-water retention capacity of two different soils under stressed-controlled condition was studied using both the stress/volume-controlled SWCC cell and filter paper tests. The soils were forced to a stress condition only in one direction, i.e. the vertical direction, and no stress whatsoever was applied during the filter paper test. The real in situ condition that the soil specimen subjected to is different from this approach. It is confined by a distinct pressure in every direction. Therefore, investigation on the effect of neglecting the stress condition in radial

direction as well as the effect of combining test results from stress/volume-controlled SWCC cell and filter paper test are recommended for future studies

2. Since it was not possible to assess the whole trend of the SWCCs for the clayey sand soil using the stress/volume-controlled SWCC cell, filter paper test was used to complete the SWCCs at a higher suction values. However, a slight divergence was observed between the points obtained from the stress/volume-controlled SWCC cell and the filter paper test. There should be some correlation to account for this divergence when combining SWCC points from these two test methods.
3. SWCC tests for both test soils was conducted following the desorption path. It is recommended too to do the SWCC test following the absorption path to assess the hysteresis of the soil-water retention properties of the test soils.

REFERENCES

Jubair Hossain, PhD (2012), "Geo-hazard potential of rainfall induced slope failure on expansive clay." The University of Texas at Arlington, 2012

Rifat Bulut, M.ASCE, Robert L. Lytton, F.ASCE, and Warren K. Wray, F.ASCE, "Soil suction measurement by filter paper." October 2001

ASTM D5298 - 10, "Standard Test Method for Measurement of Soil Potential (Suction) Using Filter Paper." Houston, Texas, 2001

ASTM D854 - 10, "Standard Test Methods for Specific Gravity of Soil Solids by Water Pycnometer."

ASTM D4318 - 10, "Standard Test Methods for Liquid Limit, Plastic Limit, and Plasticity Index of Soils."

ASTM D6913 - 04 (Reapproved 2009), "Standard Test Methods for Particle-Size Distribution" (Gradation) of Soils Using Sieve Analysis."

Ning Lu (2004), Colorado School of Mines and William J. Likos, University of Missouri-Columbia, (2004), "unsaturated soil mechanics." 2004

Fredlund, D. G. and Rahardjo, H. (1993). "Soil Mechanics for unsaturated soils." Wiley, Singapore.

Fredlund, D.G. (2006). "Unsaturated soil mechanics in engineering practice." J. Geotech. Geoenviron. Eng., 132

Fredlund, D.G., Xing, A., and Huang, S. (1994). "Predicting the permeability functions for unsaturated soils using the soil-water characteristic curve." Can. Geotech. J. Ottawa, 31, 533-546.

Fredlund, D.G., and Morgenstern, N.R., (1977). "Stress state variables for unsaturated soils." *J. Geotech. Eng.* Vol. 103, pp. 447-466.

Fredlund, D.G., Morgenstern, N.R., Wider, R.A. (1978). "Shear strength of unsaturated soils" *Canadian Geotechnical Journal*, 15(3), 313-321.

Fredlund, D. G., and Rahardjo, H. (1993). "*Soil Mechanics for unsaturated soils.*" Wiley, Singapore

Fredlund, D. G, Xing, A., Fredlund, M. D., and Barbour, S. L. (1996). "The relationship of unsaturated soil shear strength to the soil–water characteristic curve." *Can. Geotech. J.*, 33, 440–448.

Fredlund, D. G. (2006). "Unsaturated soil mechanics in engineering practice." *J. Geotech. Geoenviron. Eng.*, 132 (3), 286-321.

Gamboa, C.L.V. (2011) "Unsaturated soil behavior under large deformations using fully servo/suction controlled ring shear apparatus." PhD Thesis, The University of Texas at Arlington.

BIOGRAPHICAL INFORMATION

Hailu Ayalew graduated with a Bachelor's degree in Civil Engineering from Mekelle University, Mekelle, Ethiopia in 2007, and later on started his graduate studies at The University of Texas at Arlington in August 2011. He received his Master's degree in civil engineering with emphasis on geotechnical engineering in August 2013. Since his college graduation in 2007, he has been working in road design and construction fields. Currently, he is working for Texas Department of Transportation in Euless area office, Euless, TX. As part of his master's degree program, he worked on a project titled "Assessment of stress/volume-controlled soil-water characteristic curves of unsaturated sandy soils" under the supervision of Dr. Laureano R. Hoyos. The author's main research interest includes Foundation analysis and design, Slope stability analyses, Design of earth retaining structures, Design and construction of pavements, Site Investigation using Geophysical Method, Saturated and unsaturated Soil behaviors, and Design and construction of landfills.